HCV replicon system [3]. The replicon RNA is a selectable, bicistronic HCV RNA with the first cistron, the neomycin phosphotransferase (Neo^R) gene, being translated under control of the HCV internal ribosome entry site (IRES) and the second cistron, the NS3–NS5B regions, being translated under control of the encephalomyocarditis virus (EMCV) IRES. Therefore, we previously performed genetic analyses of HCV variation and diversity using HCV replicon systems [11, 13] developed using two HCV strains, 1B-1 and HCV-O [12]. In that study, HCV-replicon-harboring cells were cultured for 18 months (1B-1 strain) or 12 months (HCV-O strain), and, using these cell cultured specimens, the mutation rates of both HCV replicons were estimated to be approximately 3.0×10^{-3} base substitutions/site/year. The genetic diversity of both replicons was also enlarged during long-term cell cultures [12]. However, it is unclear that the obtained results reflect the variations and diversity of the whole HCV genome, since the HCV replicon lacks the core–NS2 regions (half of the HCV genome). Furthermore, information regarding the genetic variation and diversity of the core–NS2 regions is needed in order to understand the dynamics of the whole HCV genome. To clarify this point, recently established genome-length HCV RNA (HCV-O strain)-replicating cell lines, HuH-7-derived O, OA, OB, OD, and OE [1, 7], were used for this study. There is no evidence that infectious HCV particles are released into the supernatants of genome-length HCV-RNA-replicating cells (O–OE). Since genome-length HCV-RNAs possessing cell-line-specific adaptive mutations that enhance the efficiency of RNA replication efficiently replicated in these five kinds of cells, we cultured these cells for 2 years and comprehensively analyzed the variations and diversity of the whole intracellular HCV genome. Here, we report the evolutionary HCV dynamics occurring in long-term replication of genome-length HCV RNAs.

Materials and methods

Cell cultures

The O, OA, OB, OD, and OE cells supporting genome-length HCV RNAs were cultured in Dulbecco's modified Eagle's medium supplemented with fetal bovine serum (10%) and G418 (0.3 mg/ml). These cells were passaged every 7 days for 2 years.

Northern blot analysis

Total RNAs from the cultured cells were prepared using an RNeasy extraction kit (Qiagen, Hilden, Germany). Total RNA (3 μg) was used to detect the genome-length HCV RNA and β-actin mRNA (for check the amount of RNA). Northern blotting and hybridization were performed using a positive-stranded HCV-genome-specific RNA probe (NS5B region) and a β-actin-specific probe, as described previously [12].

Quantification of HCV RNA

The reverse transcription (RT)-quantitative PCR (RT-qPCR) analysis for HCV RNA was performed using LightCycler PCR as described previously [8]. Experiments were done in triplicate.

Western blot analysis

The preparation of cell lysates, SDS-PAGE, and immunoblotting analysis with a PVDF membrane were performed as described previously [6]. The antibodies used to examine the expression levels of HCV proteins were those against core [CP9, CP11, and CP14 monoclonal antibodies (Institute of Immunology, Tokyo); a polyclonal antibody (a generous gift from Dr. M. Kohara, Tokyo Metropolitan Institute of Medical Science, Japan)], E1 and NS5B (generous gifts from Dr. M. Kohara, Tokyo Metropolitan Institute of Medical Science, Japan). The epitopes of CP9, CP11, and CP14 were located within aa positions 39–74, 21–40, and 5–40 of the core protein, respectively. Anti-β-actin antibody (AC-15; Sigma, St. Louis, MO) was also used to detect β-actin as an internal control. Immunocomplexes on the membranes were detected by enhanced chemiluminescence assay (Renaissance; Perkin-Elmer Life Sciences, Boston, MA).

RT-PCR and sequencing

To amplify genome-length HCV RNA, RT-PCR was performed separately in two fragments as described previously [7]. Briefly, one fragment covered from 5′-UTR to NS3, with a final product of approximately 5.1 kb, and the other fragment covered from NS2 to NS5B, with a final product of approximately 6.1 kb. These fragments overlapped at the NS2 and NS3 regions and were used for sequence analysis of the HCV open reading frame (ORF) after cloning into pBR322MC [11]. SuperScript II (Invitrogen, Carlsbad, CA) and KOD-plus DNA polymerase (Toyobo, Osaka, Japan) were used for RT and PCR, respectively. Plasmid inserts were sequenced in both the sense and antisense directions using Big Dye terminator cycle sequencing on an ABI PRISM 310 genetic analyzer (Applied Biosystems, Foster City, CA). The nucleotide sequences of each of the three independent clones obtained were determined.

Molecular evolutionary analysis

Nucleotide and deduced amino acid sequences of the clones obtained by RT-PCRs were analyzed by neighbor-joining analysis using the program GENETYX-MAC (Software Development, Tokyo, Japan).

Results

Efficient replication of genome-length HCV RNA is maintained in long-term cell culture

To prepare the specimens for the genetic analysis of HCV, genome-length HCV-RNA-replicating O, OA, OB, OD, and OE cells were cultured for 2 years. The cell-line-specific and conserved adaptive mutations, K1609E, E1202G, P1115L, Q1112R, and P1115L, in the NS3 region were detected in the O, OA, OB, OD, and OE cells, respectively, when these cell lines were established [1, 7]. Using the specimens obtained at 0, 1, and 2 years in culture of O, OA, OB, OD, and OE cells, the levels of genome-length HCV RNAs were examined by Northern blot analysis (Fig. 1a) and RT-qPCR analysis (Fig. 1b). As shown in Fig. 1a, genome-length HCV RNAs approximately 11 kb long were detected in all specimens except that from HuH-7 parental cells, although the strength of the detected bands was weak in some cases. However, RT-qPCR analysis revealed that at least approximately 2×10^7 copies/μg RNA were present in the cultured cells (Fig. 1b). The results of RT-qPCR were well correlated with those of Northern blot analysis. The levels of HCV proteins (core, E1, and NS5B) were also examined by Western blot analysis. The E1 and NS5B proteins were also detected in all specimens except that from HuH-7 cells, although the levels of E1 protein were rather different among the specimens (Fig. 1c). In contrast, core protein was not detected in OB1, OB2, and OE2 cells, when the mixture of three kinds of monoclonal antibodies (CP9, CP11, and CP14) was used for the analysis. Even when polyclonal anti-core antibody was used, core protein was still not detected in OB2 cells. In addition, the strength of bands detected in the Western blot analysis was decreased in a time-dependent manner. These results suggest that sequence variations within the epitopes of the anti-core or E1 antibody, but not the anti-NS5B antibody, have occurred during the long-term cell culture.

Genetic variations of genome-length HCV RNAs during long-term cell culture

The determined nucleotide sequences of genome-length HCV RNAs were compared with those of the original ON/C-5B RNA (Gene Bank accession no. AB191333) [7] used for the establishment of the O, OA, OB, OD, and OE cell lines. The results revealed that the numbers of base substitutions in genome-length HCV RNAs increased in a time-dependent manner (Fig. 2). These substitutions were considered to be mutations that occurred during the intracellular replication of genome-length HCV RNA. Based on the results after 2 years in culture, the apparent mutation rates of genome-length HCV RNAs in O, OA, OB, OD, and OE cells were calculated to be 3.5 ± 0.4, 4.5 ± 1.4, 4.8 ± 0.6, 4.3 ± 0.5, $4.2 \pm 0.4 \times 10^{-3}$ base substitutions/site/year, respectively. These values suggest that the genetic evolution of HCV in these different cell lines occurs at similar rates during long-term RNA replication. The deduced aa substitution rates in HCV ORFs among these cell lines are well correlated with the mutation rates of HCV RNAs (Fig. 2). We further examined whether or not the mutation rates are similar throughout the HCV genome. For this analysis, genome-length HCV RNA was divided into three parts: the 5′-terminus to the EMCV IRES region (1,938 nts), the core to the NS2 region (3,078 nts), and the NS3 to the NS5B region (5,955 nts). The results revealed that the mutation rates in the NS3–NS5B regions were lower than those of the other regions, although the 5′-terminus to the EMCV IRES region in the OA and OE cell lines showed mutation rates similar to that for the NS3–NS5B regions (Fig. 3). These results suggest that the NS3–NS5B regions, which are essential for RNA replication, are evolutionally limited. The conserved aa substitutions (mutated in all three clones sequenced) are summarized in Table 1 (core–p7 regions) and Table 2 (NS2–NS5B regions). Eight aa substitutions (K12N, Q1112R, P1115L, K1609E, A1738T, K2280E, D2292E, and D2415G) were commonly detected in at least two different cell lines. Approximately 57% of aa substitutions detected in this study were found in the Hepatitis Virus Database (http://s2as02.genes.nig.ac.jp; Nagoya City University, Japan).

Classification of mutations occurring in genome-length HCV RNAs during the long-term cell culture

We examined the numbers of synonymous and non-synonymous mutations with transition or transversion in three divided regions (Neo^R, core–NS2, and NS3–NS5B regions). The results revealed that the frequencies of aa substitutions in the NS3–NS5B regions were lower than those in the core–NS2 regions, and that the rate of transition mutations in genome-length HCV RNA was greater than the rate of transversion mutations (Supplementary Table S1), as previously reported for the replicon system [12].

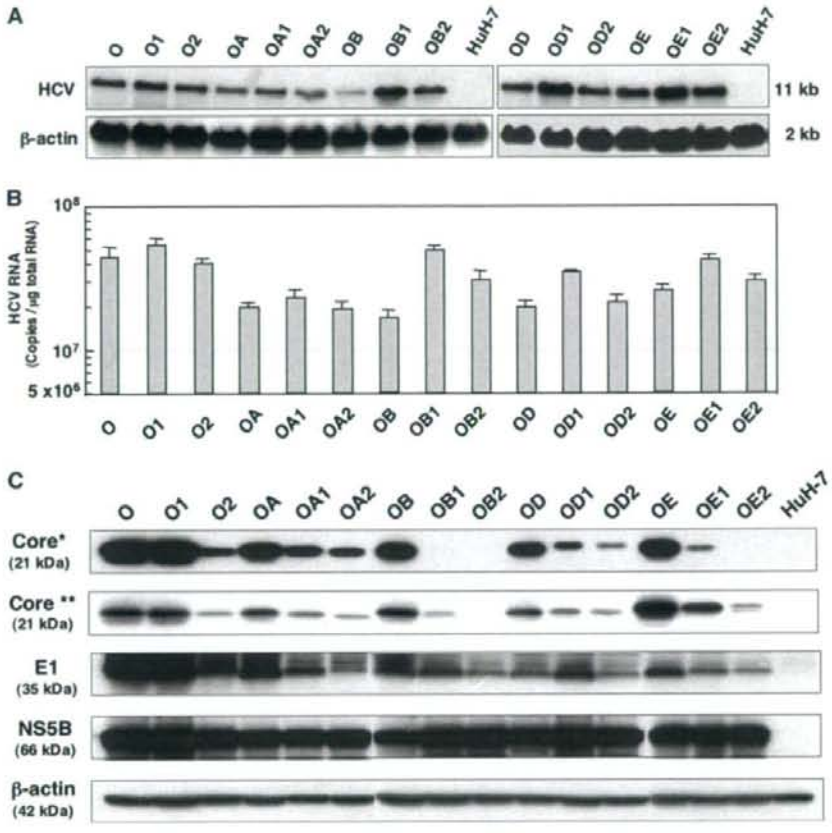

Fig. 1 Characterization of cells containing replicating genome-length HCV RNA in long-term cell culture. **a** Northern blot analysis. Total RNAs from O, OA, OB, OD, and OE cells after 1 year (O1, OA1, OB1, OD1, and OE1) and 2 years (O2, OA2, OB2, OD2, and OE2) in culture, as well as total RNAs from the parental O, OA, OB, OD, and OE cells were used for the analysis. HuH-7 cells were used as a negative control. In vitro-synthesized ON/C-5B RNA [1] was used as a size marker (11 kb). **b** Quantitative analysis of intracellular genome-length HCV RNA. The total RNAs from the cells used for Northern blot analysis were also used for comparison. The levels of intracellular genome-length HCV RNA were quantified by Light-Cycler PCR. **c** Western blot analysis. The cellular lysates from the cells used for Northern blot analysis were also used for comparison. Core, E1, and NS5B were detected by Western blot analysis. β-actin was used as a control for the amount of protein loaded per lane. A *single star* indicates that the mixture of three kinds (CP9, CP11, and CP14) of anti-core monoclonal antibodies was used for detection. A *double star* indicates that the anti-core polyclonal antibody was used for detection

Also regarding the mutation patterns, U → C and A → G mutations were the most and second-most frequent mutations, and these mutations were two to three times more frequent than C → U and G → A mutations (Supplementary Table S2) as previously reported in the replicon analysis [12]. The rarest mutation was C → G in 1- and 2-year cultures (Supplementary Table S2). As a result, we observed that the GC content of HCV RNA gradually increased in a time-dependent manner. The increase in GC content was observed in all genome-length HCV RNAs obtained from cultured cell lines (Fig. 4).

Genetic diversity of genome-length HCV RNA arising during long-term cell culture

Based on the sequence data of all clones obtained after 2-year culture, we examined the genetic diversities of genome-length HCV RNAs by the construction of phylogenetic trees. The results revealed that the genetic diversities of genome-length HCV RNAs were expanded at both the nucleotide and aa sequence levels, as previously reported in the replicon analysis [12], and that the three clones derived from each cell line were clustered and located at similar genetic distances from the origin

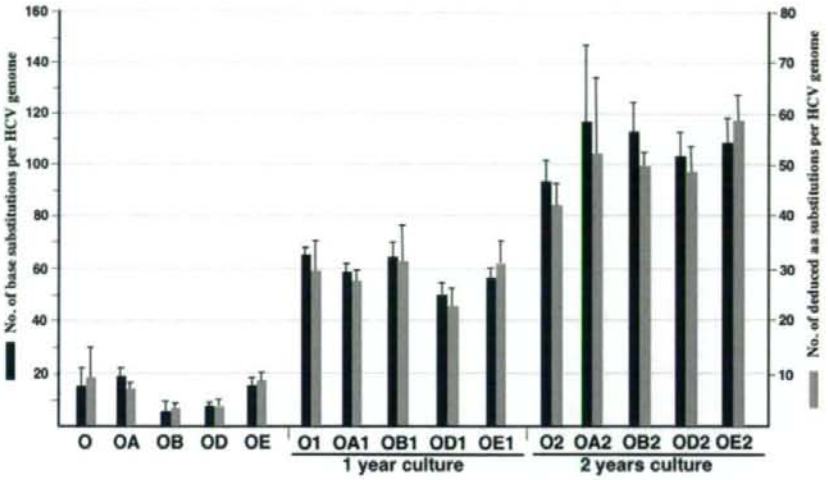

Fig. 2 Genetic variations occurring in long-term replication of genome-length HCV RNAs. The *left vertical line* indicates the mean numbers of base substitutions detected in three clones of genome-length HCV RNA, by comparison with the original sequences (ON/C-5B) [7]. The *right vertical line* indicates the mean numbers of aa substitutions deduced from each of three clones of genome-length HCV RNA, by comparison with the original aa sequences (ON/C-5B) [7]

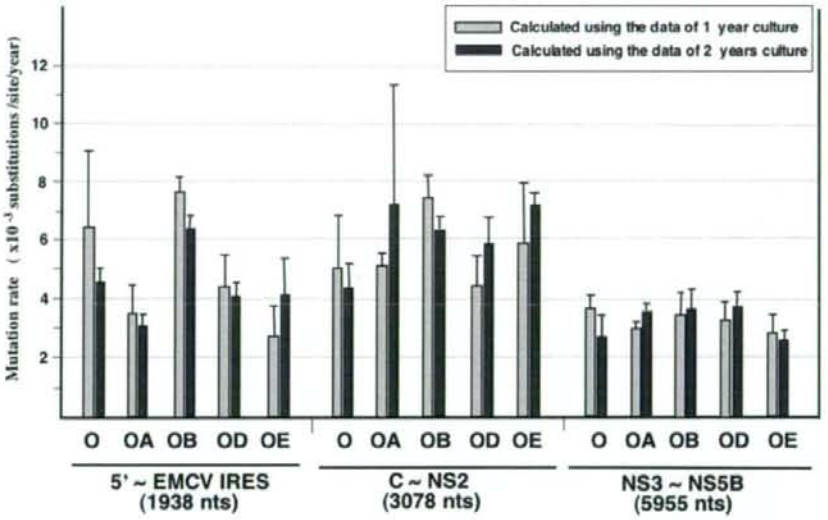

Fig. 3 Mutation rates of genome-length HCV RNAs in long-term cell culture. The mutation rates of three regions (5′–EMCV-IRES, Core–NS2, and NS3–NS5B) of genome-length HCV RNAs (O, OA, OB, OD, and OE) were calculated using the sequence data obtained from 1- or 2-year cell culture. The *vertical line* indicates the means of the mutation rates calculated using the nucleotide sequences of three clones of genome-length HCV RNAs, by comparison with the original sequences (ON/C-5B) [7]

(ON/C-5B) at both the nucleotide and aa sequence level (Supplementary Fig. S1). These results indicate that the quasispecies nature of genome-length HCV RNA has been steadily acquired over long-term intracellular RNA replication.

Discussion

In the present study, we analyzed the genetic evolution and dynamics of HCV in long-term culture of five kinds of genome-length HCV-RNA-replicating cells, and demonstrated that the genetic mutations of HCV accumulated in a time-dependent manner, and the genetic diversity of HCV also increased with time. These results will be useful for understanding the quasispecies nature of HCV in patients with chronic hepatitis C.

Previously, we reported that the genetic mutation rate of HCV replicons (subgenomic RNA) was approximately 3.0×10^{-3} base substitutions/site/year in both the 5′ terminus–EMCV IRES region and the NS3–NS5B regions [12]. The NS3–NS5B regions in this study showed mutation rates ($2.8–3.8 \times 10^{-3}$ base substitutions/site/year) similar to those of the replicons in the previous study; however, the mutation rates of the 5′ terminus to the EMCV IRES region in O and OB cells were over 6.0×10^{-3} base substitutions/site/year, suggesting that genetic mutations in this region occur independently

Table 1 Conserved aa substitutions occurring during long-term replication of genome-length HCV RNAs (I)

Region	aa Substitution	Observed cells	Region	aa Substitution	Observed cells	Region	aa Substitution	Observed cells
Core	S2G	OB2	Core	N163S	O2	E2	A457T[a]	OB1, OB2
	K6N	OB2		N163T	OE1, OE2		D463H[a]	OE, OE1, OE2
	K10R[a]	OB2		L169S	OD1, OD2		W469R	OE2
	K10E	OA2		F174S	O2		Y485H	OA1, OA2
	K12N[a]	OA1, OA2		F177S	OB1, OB2		Y485C	OD2
		OE2					G504S	OE2
	N16D	OE1, OE2	E1	N205T	O2		Y507H	OA2
	F24V	OB2		D218G[a]	OB2		L537P	OB2
	V34A	OD2		M219V[a]	OB1, OB2		M555V[a]	OB1
	R40G	O2		I220V[a]	OE1, OE2		T595A[a]	OA2
	L44M[a]	OE2		C226R[a]	OE2		K595A[a]	OA2
	T49A[a]	OE2		L242I[a]	OE2		K596N	OD1, OD2
	K67M[a]	O2		T257A[a]	OA1, OA2		L603S	OE2
	P71S[a]	O2		I258K	OE, OE1, OE2		C607S	OA1, OA2
	A75P	OE2		L264S[a]	O2		G649E	OE2
	A77T	OB2		C272R[a]	OE2		D658G[a]	OD1, OD2
	A77P	OD2		S273P[a]	O2		T670A[a]	OB2
	E89V[a]	O2		R296H[a]	OD1		I674T[a]	O2
	R101C	OE2		Q302R[a]	OA1, OA2		L689S	OA1, OA2
	T110M[a]	OE1, OE2		V313A[a]	OB2		N695S	OE2
	L119S	OB2		Y361C[a]	OA2		V713L	OA1, OA2
	K121R	OD1, OD2		Y361H	OE, OE1, OE2		Y718H	OB1, OB2
	I123T[a]	O2		V381D	OA2		Y718C	OD1
	F130L[a]	OA1, OA2					L722P	O2
	L133F	OB2	E2	G389R	OE2			
	L139P	OE1, OE2		F437S	OD1, OD2	p7	F771S	OE2
							L796P	O2

[a] aa Substitutions found in the Hepatitis Virus Databasse (http://s2as02.genes.nig.ac.jp; Nagoya City University, Japan)

among these cell lines. It was also noticed that the mutation rates ($4.3–7.4 \times 10^{-3}$ base substitutions/site/year) in the core–NS2 regions became higher than those in the NS3–NS5B regions due to frequent mutations in the core, E1, and E2 regions (Table 1). It was particularly difficult to detect the core protein by Western blot analysis due to the genetic changes within epitopes for anti-core antibodies (Fig. 1c). These results suggest that the structural region including the core, E1, and E2 regions is not required for persistent intracellular RNA replication, although approximately 42% of the aa substitutions detected in this study were observed in HCV-infected persons (Table 1). However, since we have recently found that DDX3 DEAD-box RNA helicase, which binds to the N-terminal domain (aa 1–59) of the core protein, is required for efficient replication of genome-length HCV RNA in O cells [2], none of the mutations detected in the core region should impair the interaction with DDX3. Furthermore, 6 and 9N-glycosylation sites in the E1 and E2 proteins, respectively, were completely conserved even after 2 years in culture, indicating that the E1 and E2 proteins may also affect the efficiency of RNA replication. Therefore, we speculate that the aa substitutions detected in the structural region do not reflect all of the random mutations occurring in long-term RNA replication. In contrast to the numerous aa substitutions in the structural region, the hypervariable region (HVR) 1 located in the N-terminal region of the E2 protein showed only one aa substitution (G389R in OE2 cells). This finding supports our previous proposition that an immunosurveillance system is involved in the genetic mutation in HVR1 [10]. In addition, no aa substitutions were detected in HVR2 (aa 474–480) of the E2 protein.

We showed that the mutation rates of HCV RNAs were $3.5–4.8 \times 10^{-3}$ base substitutions/site/year. However, our observed mutation rates of the HCV RNAs were 1.8–3.4 times higher than those previously obtained in chimpanzees [16, 18] and a human patient [17] with chronic hepatitis C. Since the selective pressures of the humoral immune responses [10] targeting the envelope proteins and cellular immune responses [24] targeting all HCV proteins

Table 2 Conserved aa substitutions occurring during long-term replication of genome-length HCV RNAs (II)

Region	aa Substitution	Observed cells	Region	aa Substitution	Observed cells	Region	aa Substitution	Observed cells
NS2	M814T[a]	OE1, OE2	NS4B	L1724I[a]	OB2	NS5A	D2377G[a]	OA2
	I885V[a]	O2		A1738T[a]	OA2		V2385H[a]	OD2
	F886L	OB2			OD1, OD2		S2387P	OD1, OD2
	E887G[a]	O2			OE2		L2391P	OA2
	T889A	OB2		I1797V[a]	OB2		W2405R[a]	OE2
	I891V[a]	O2		P1822S	OE2		E2414G[a]	OB2
	L902F[a]	OB2		V1880A	OA1, OA2		D2415G[a]	OA, OA1, OA2
	M939V[a]	OE, OE1, OE2						OD1, OD2
			NS5A	S1975T[a]	OE2		C2418R[a]	OA2
NS3	Q1112R[a, b]	O1, O2		H2218R[a]	OE2			
		OB2		H2219R[a]	OB2	NS5B	N2529S[a]	OB2
		OD, OD1, OD2		S2221F[a]	OA2		N2536S[a]	OB2
	P1115L[a, b]	OB, OB1, OB2		N2248D[a]	OB2		V2757A[a]	OB2
		OE, OE2		K2280E[a]	OB2		K2860R[a]	OB2
	N1148S[a]	OE2			OD1, OD2		R2963Q[a]	OB2
	E1202G[a, b]	OA, OA1, OA2		A2284T	OB2		W2990R	O2
	T1531A[a]	OA2		D2292E[a]	OB2		V3002A	O2
	D1581E[a]	OA2			OE2			
	K1609E[a, b]	O, O1, O2		V2340M[a]	OA2			
		OE2		S2342P[a]	OD2			
	I1612T[a]	OD1, OD2		G2371A[a]	OE2			
	I1641M[a]	OD1, OD2		G2376S[a]	OD1, OD2			

[a] aa Substitutions found in the Hepatitis Virus Database (http://s2as02.genes.nig.ac.jp; Nagoya City University, Japan)

[b] Adaptive mutations detected in O, OA, OB, OD, and OE cells when these cell lines were established [1, 7]

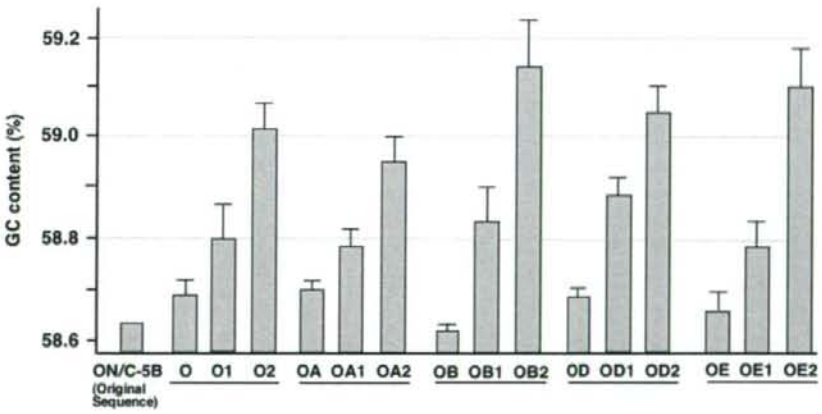

Fig. 4 Increased GC content of genome-length HCV RNAs in long-term cell culture. The GC content of genome-length HCV RNAs (O–O2, OA–OA2, OB–OB2, OD–OD2, and OE–OE2) was calculated. The values indicate the means of three clones of each genome-length HCV RNA

function in vivo, the mutation rates obtained in this study using the cell culture system without the immunological pressure would be reasonable values as a potential mutation rate of HCV in RNA replication.

It is noteworthy that none of the aa substitutions were detected in the N-terminal half (242 aa of aa 1,976–2,217) of the NS5A protein after 2 years in cell cultures. This finding suggests that this region is the most critical for maintenance of RNA replication. It is interesting that this region corresponds to domain I (aa 1,973–2,185), which has been shown to complex with a zinc ion [21] and exists as a dimer [22]. Since the mutation of four cysteine residues essential for binding to zinc ions results in the complete inhibition of RNA replication [21], the complete

conservation of domain I in this study suggests that the intact form of domain I is required for efficient RNA replication. Genetic analysis in further long-term cell cultures will specifically clarify the critical domains required for the maintenance of RNA replication.

The unexpected phenomenon in this study was the time-dependent increase of the GC content of the HCV genome. After 1 year in culture, the GC content increased 0.14% (mean of five cell culture lines), corresponding to 15 nts per HCV genome, and during the next 1 year in culture, the GC content increased an additional 0.24% (mean of five cell culture lines), corresponding to 26 nts per HCV genome. Consequently, approximately 40 nts per HCV genome changed to a G or C residue during the 2 years in culture. The HCV genome may gradually change to an energetically stable form during RNA replication. The other possibility is that the increase in GC content may be due to an increase in G- and C-ending codons, except AGG and TTG codons, for efficient expression in human cells (codon optimization) [14]. However, our study revealed that the increase of G- and C-ending codons other than codons AGG and TTG was only 16–18% of the increase of GC content observed during the 2-year cultures of O–OE cells. To understand the mechanism underlying the increase of the GC content of genome-length HCV RNA during long-term RNA replication, further long-term cell cultures will be needed.

This study demonstrated that a single HCV genome could exhibit a quasispecies nature after 2 years in cell culture with RNA replication. Such quasispecies populations of HCV obtained by long-term cell culture may be useful not only for further analysis of the genetic variations and diversity of HCV but also for analysis of the sensitivity of reagents such as interferon against HCV.

Acknowledgments We thank T. Nakamura for his technical assistance. This work was supported by a grant-in-aid for the third-term comprehensive 10-year strategy for cancer control and by a grant-in-aid for research on hepatitis, both from the Ministry of Health, Labor, and Welfare of Japan.

References

1. Abe K, Ikeda M, Dansako H, Naka K, Kato N (2007) Cell culture-adaptive NS3 mutations required for the robust replication of genome-length hepatitis C virus RNA. Virus Res 125:88–97
2. Ariumi Y, Kuroki M, Abe K, Dansako H, Ikeda M, Wakita T, Kato N (2007) DDX3 DEAD-box RNA helicase is required for hepatitis C virus RNA replication. J Virol 81:13922–13926
3. Bartenschlager R (2005) The hepatitis C virus replicon system: from basic research to clinical application. J Hepatol 43:210–216
4. Bukh J, Miller RH, Purcell RH (1995) Genetic heterogeneity of hepatitis C virus: quasispecies and genotypes. Semin Liver Dis 15:41–63
5. Hijikata M, Kato N, Ootsuyama Y, Nakagawa M, Shimotohno K (1991) Gene mapping of the putative structural region of the hepatitis C virus genome by in vitro processing analysis. Proc Natl Acad Sci USA 88:5547–5551
6. Hijikata M, Mizushima H, Tanji Y, Komoda Y, Hirowatari Y, Akagi T, Kato N, Kimura K, Shimotohno K (1993) Proteolytic processing and membrane association of putative nonstructural proteins of hepatitis C virus. Proc Natl Acad Sci USA 90:10773–10777
7. Ikeda M, Abe K, Dansako H, Nakamura T, Naka K, Kato N (2005) Efficient replication of a full-length hepatitis C virus genome, strain O, in cell culture, and development of a luciferase reporter system. Biochem Biophys Res Commun 329:1350–1359
8. Kato N (2001) Molecular virology of hepatitis C virus. Acta Med Okayama 55:133–159
9. Kato N, Hijikata M, Ootsuyama Y, Nakagawa M, Ohkoshi S, Sugimura T, Shimotohno K (1990) Molecular cloning of the human hepatitis C virus genome from Japanese patients with non-A, non-B hepatitis. Proc Natl Acad Sci USA 87:9524–9528
10. Kato N, Sekiya H, Ootsuyama Y, Nakazawa T, Hijikata M, Ohkoshi S, Shimotohno K (1993) Humoral immune response to hypervariable region 1 of the putative envelope glycoprotein (gp70) of hepatitis C virus. J Virol 67:3923–3930
11. Kato N, Sugiyama K, Namba K, Dansako H, Nakamura T, Takami M, Naka K, Nozaki A, Shimotohno K (2003) Establishment of a hepatitis C virus subgenomic replicon derived from human hepatocytes infected in vitro. Biochem Biophys Res Commun 306:756–766
12. Kato N, Nakamura T, Dansako H, Namba K, Abe K, Nozaki A, Naka K, Ikeda M, Shimotohno K (2005) Genetic variation and dynamics of hepatitis C virus replicons in long-term cell culture. J Gen Virol 86:645–656
13. Kishine H, Sugiyama K, Hijikata M, Kato N, Takahashi H, Noshi T, Nio Y, Hosaka M, Miyanari Y, Shimotohno K (2002) Subgenomic replicon derived from a cell line infected with the hepatitis C virus. Biochem Biophys Res Commun 293:993–999
14. Kliman RM, Bernal CA (2005) Unusual usage of AGG and TTG codons in humans and their viruses. Gene 352:92–99
15. Lohmann V, Korner F, Koch J, Herian U, Theilmann L, Bartenschlager R (1999) Replication of subgenomic hepatitis C virus RNAs in a hepatoma cell line. Science 285:110–113
16. Major ME, Mihalik K, Fernandez J, Seidman J, Kleiner D, Kolykhalov A, Rice CM, Feinstone SM (1999) Long-term follow-up of chimpanzees inoculated with the first infectious clone for hepatitis C virus. J Virol 73:3317–3325
17. Ogata N, Alter HJ, Miller RH, Purcell RH (1991) Nucleotide sequence and mutation rate of the H strain of hepatitis C virus. Proc Natl Acad Sci USA 88:3392–3396
18. Okamoto H, Kojima M, Okada S, Yoshizawa H, Iizuka H, Tanaka T, Muchmore EE, Peterson DA, Ito Y, Mishiro S (1992) Genetic drift of hepatitis C virus during an 8.2-year infection in a chimpanzee: variability and stability. Virology 190:894–899
19. Simmonds P (2004) Genetic diversity and evolution of hepatitis C virus—15 years on. J Gen Virol 85:3173–3188
20. Tanaka T, Kato N, Nakagawa M, Ootsuyama Y, Cho MJ, Nakazawa T, Hijikata M, Ishimura Y, Shimotohno K (1992) Molecular cloning of hepatitis C virus genome from a single Japanese carrier: sequence variation within the same individual and among infected individuals. Virus Res 23:39–53
21. Tellinghuisen TL, Marcotrigiano J, Gorbalenya AE, Rice CM (2004) The NS5A protein of hepatitis C virus is a zinc metalloprotein. J Biol Chem 279:48576–48587
22. Tellinghuisen TL, Marcotrigiano J, Rice CM (2005) Structure of the zinc-binding domain of an essential component of the hepatitis C virus replicase. Nature 435:374–379

23. Thomas DL (2000) Hepatitis C epidemiology. Curr Top Microbiol Immunol 242:25–41
24. Weiner A, Erickson AL, Kansopon J, Crawford K, Muchmore E, Hughes AL, Houghton M, Walker CM (1995) Persistent hepatitis C virus infection in a chimpanzee is associated with emergence of a cytotoxic T lymphocyte escape variant. Proc Natl Acad Sci USA 92:2755–2759

JOURNAL OF VIROLOGY, Oct. 2008, p. 9639–9646 Vol. 82, No. 19
0022-538X/08/$08.00+0 doi:10.1128/JVI.00351-08

The DNA Damage Sensors Ataxia-Telangiectasia Mutated Kinase and Checkpoint Kinase 2 Are Required for Hepatitis C Virus RNA Replication▽

Yasuo Ariumi,[1] Misao Kuroki,[1] Hiromichi Dansako,[1] Ken-Ichi Abe,[1] Masanori Ikeda,[1] Takaji Wakita,[2] and Nobuyuki Kato[1]*

Department of Molecular Biology, Okayama University Graduate School of Medicine, Dentistry, and Pharmaceutical Sciences, 2-5-1, Shikata-cho, Okayama 700-8558, Japan,[1] and Department of Virology II, National Institute of Infectious Diseases, 1-23-1 Toyama, Shinjuku-ku, Tokyo 162-8640, Japan[2]

Received 18 February 2008/Accepted 18 July 2008

Cellular responses to DNA damage are crucial for maintaining genome integrity, virus infection, and preventing the development of cancer. Hepatitis C virus (HCV) infection and the expression of the HCV nonstructural protein NS3 and core protein have been proposed as factors involved in the induction of double-stranded DNA breaks and enhancement of the mutation frequency of cellular genes. Since DNA damage sensors, such as the ataxia-telangiectasia mutated kinase (ATM), ATM- and Rad3-related kinase (ATR), poly(ADP-ribose) polymerase 1 (PARP-1), and checkpoint kinase 2 (Chk2), play central roles in the response to genotoxic stress, we hypothesized that these sensors might affect HCV replication. To test this hypothesis, we examined the level of HCV RNA in HuH-7-derived cells stably expressing short hairpin RNA targeted to ATM, ATR, PARP-1, or Chk2. Consequently, we found that replication of both genome-length HCV RNA (HCV-O, genotype 1b) and the subgenomic replicon RNA were notably suppressed in ATM- or Chk2-knockdown cells. In addition, the RNA replication of HCV-JFH1 (genotype 2a) and the release of core protein into the culture supernatants were suppressed in these knockdown cells after inoculation of the cell culture-generated HCV. Consistent with these observations, ATM kinase inhibitor could suppress the HCV RNA replication. Furthermore, we observed that HCV NS3-NS4A interacted with ATM and that HCV NS5B interacted with both ATM and Chk2. Taken together, these results suggest that the ATM signaling pathway is critical for HCV RNA replication and may represent a novel target for the clinical treatment of patients with chronic hepatitis C.

Hepatitis C virus (HCV) infection frequently causes chronic hepatitis, which progresses to liver cirrhosis and hepatocellular carcinoma. HCV infection has now become a serious health problem, with at least 170 million people currently infected worldwide (28). HCV is an enveloped virus with a positive single-stranded 9.6-kb RNA genome, which encodes a large polyprotein precursor of approximately 3,000 amino acid residues. This polyprotein is cleaved by a combination of the host and viral proteases into at least 10 proteins in the following order: core, envelope 1 (E1), E2, p7, nonstructural 2 (NS2), NS3, NS4A, NS4B, NS5A, and NS5B (12, 13, 27).

Studies have shown that various viruses with distinct replication strategies—including the DNA viruses Epstein-Barr virus, herpes simplex virus 1, adenovirus, and simian virus 40 and the retrovirus human immunodeficiency virus type 1 (HIV-1)—can activate DNA damage response pathways and utilize these damage responses to facilitate their own viral reproduction and promote the survival of infected cells (2, 16, 17). In the case of HCV, it has been proposed that HCV infection causes double-stranded DNA (dsDNA) breaks and enhances the mutation frequency of cellular genes and that these effects are mediated by nitric oxide (18, 19). In addition, the HCV core, E1, and NS3 proteins have been suggested to be potent reactive oxygen species inducers, leading to DNA damage (19). Furthermore, we previously demonstrated that HCV NS5B-expressing PH5CH8 immortalized human hepatocyte cells were susceptible to DNA damage in the form of dsDNA breaks (23). Thus, HCV seems to be associated with the dsDNA damage response pathways.

Since the DNA damage sensors, such as ataxia-telangiectasia mutated kinase (ATM), ATM- and Rad3-related kinase (ATR), poly(ADP-ribose) polymerase 1 (PARP-1), and checkpoint kinase 2 (Chk2; a direct downstream target of ATM), play central roles in response to genotoxic stress (10), we hypothesized that these sensors might affect HCV replication.

To investigate the possible involvement of these cellular factors in HCV replication, we examined the level of HCV RNA in cells rendered defective for DNA damage sensors by RNA interference or by pharmacological inhibition.

MATERIALS AND METHODS

Cell culture. 293FT cells were cultured in Dulbecco's modified Eagle's medium (DMEM; Invitrogen, Carlsbad, CA) supplemented with 10% fetal bovine serum (FBS). The HuH-7-derived O cells harboring a replicative genome-length HCV RNA and the HuH-7-derived sO cells harboring the subgenomic replicon RNA of HCV-O were cultured in DMEM with 10% FBS and G418 (300 μg/ml geneticin; Invitrogen) as described previously (11, 14). Oc and sOc cells, which were created by eliminating HCV RNA from O cells and sO cells by interferon (IFN) treatment (11, 14), respectively, were also cultured in DMEM with 10% FBS.

RNA interference. Oligonucleotides with the following sense and antisense sequences were used for the cloning of short hairpin RNA (shRNA)-encoding se-

* Corresponding author. Mailing address: Department of Molecular Biology, Okayama University Graduate School of Medicine, Dentistry, and Pharmaceutical Sciences, 2-5-1, Shikata-cho, Okayama 700-8558, Japan. Phone: 81 86 235 7385. Fax: 81 86 235 7392. E-mail: nkato@md.okayama-u.ac.jp.

▽ Published ahead of print on 30 July 2008.

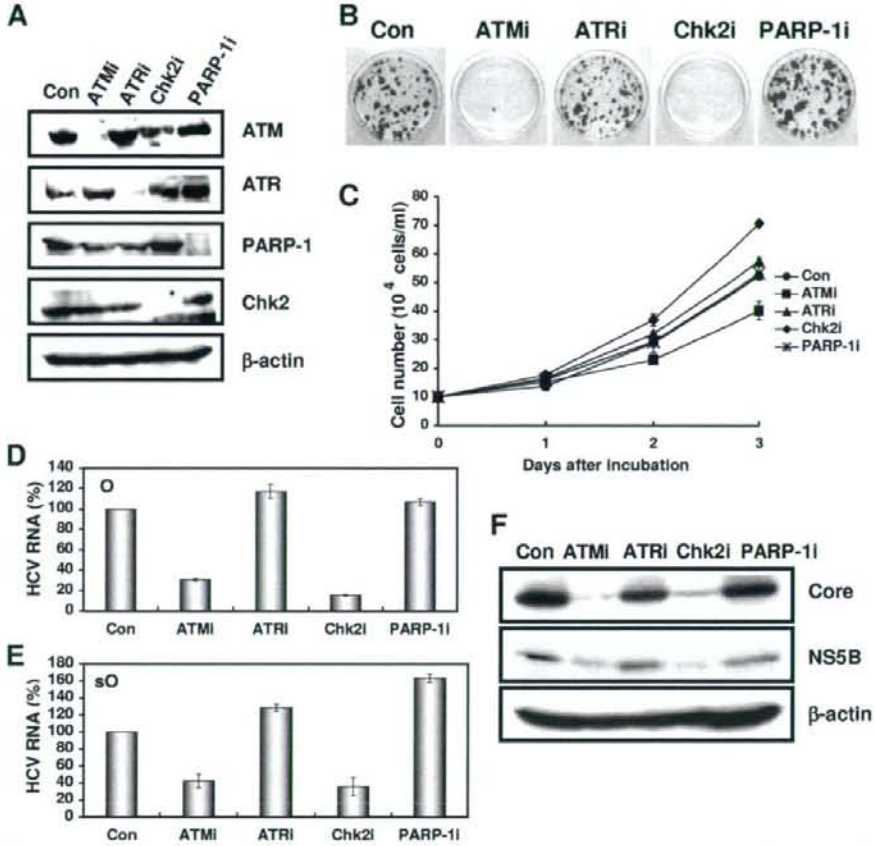

FIG. 1. The ATM signaling pathway is required for HCV RNA replication. (A) Inhibition of ATM, ATR, Chk2, or PARP-1 expression by shRNA-producing lentiviral vectors. The results of the Western blot analysis of cellular lysates with anti-ATM, anti-ATR, anti-Chk2, anti-PARP-1, or anti-β-actin antibody in Oc cells expressing shRNA targeted to ATM (ATMi), ATR (ATRi), Chk2 (Chk2i), or PARP-1 (PARP-1i) as well as in Oc cells transduced with a control lentiviral vector (Con) are shown. (B) ECF in ATM-, ATR-, Chk2-, or PARP-1-knockdown cells. In vitro transcribed ON/C-5B K1609E RNA (2 μg) was transfected into the ATM-, ATR-, Chk2, or PARP-1-knockdown Oc cells or the Oc cells transduced with a control lentiviral vector (Con). G418-resistant colonies were stained with Coomassie brilliant blue at 3 weeks after electroporation of RNA. Experiments were done in duplicate, and a representative result is shown. (C) The cell growth curve of ATM (ATMi), ATR (ATRi), Chk2 (Chk2i), or PARP-1 (PARP-1i)-knockdown Oc cells or the Oc cells transduced with a control lentiviral vector (Con). Results from three independent experiments are shown. (D) The level of genome-length HCV-O RNA was monitored by real-time LightCycler PCR (Roche). Experiments were done in triplicate, and columns represent the mean percentage of HCV RNA. (E) The level of subgenomic replicon (sO cells) RNA was monitored by real-time LightCycler PCR. Results from three independent experiments are shown as described in panel D. (F) The HCV core or NS5B protein expression level in ATM-, ATR-, Chk2-, or PARP-1-knockdown cells. The results of Western blot analysis of cellular lysates with anti-HCV core protein, anti-HCV NS5B, or anti-β-actin antibody in O cells expressing shRNA targeted to ATM (ATMi), ATR (ATRi), Chk2 (Chk2i), or PARP-1 (PARP-1i) as well as in O cells transduced with a control lentiviral vector (Con) are shown.

quences targeted to Chk2 in lentiviral vector: 5′-GATCCCCGGGGGAGAGCTGTT TGACATTCAAGAGATGTCAAACAGCTCTCCCCCTTTTTGGAAA-3′ (sense) and 5′-AGCTTTTCCAAAAAGGGGGAGAGCTGTTTGACATCTCTTGAATGT CAAACAGCTCTCCCCCGGG-3′ (antisense). The oligonucleotides above were annealed and subcloned into the BglII-HindIII site, downstream from an RNA polymerase III promoter of pSUPER (5), generating pSUPER-Chk2i. To construct pLV-Chk2i, the BamHI-SalI fragments of the pSUPER-Chk2i were subcloned into the BamHI-SalI site of pRDI292, an HIV-1-derived self-inactivating lentiviral vector containing a puromycin resistance marker allowing for the selection of transduced cells (4). pLV-ATMi, pLV-ATRi, and pLV-PARP-1i were constructed as described previously (1).

Lentiviral vector production. The vesicular stomatitis virus G protein (VSV-G)-pseudotyped HIV-1-based vector system has been described previously (24). The lentiviral vector particles were produced by transient transfection of the second-generation packaging construct pCMV-ΔR8.91 (30) and the VSV-G envelope plasmid pMDG2 as well as the lentiviral vector into 293FT cells with FuGene6 (Roche Diagnostics, Mannheim, Germany).

Quantitative reverse transcription-PCR analysis. Quantitative reverse transcription-PCR analysis for HCV RNA was performed by real-time LightCycler PCR as described previously (11).

Western blot analysis. Cells were lysed in buffer containing 50 mM Tris-HCl (pH 8.0), 150 mM NaCl, 4 mM EDTA, 1% Nonidet P-40, 0.1% sodium dodecyl sulfate (SDS), 1 mM dithiothreitol, and 1 mM phenylmethylsulfonyl fluoride. Supernatants from these lysates were subjected to SDS-polyacrylamide gel electrophoresis, followed by immunoblotting analysis using anti-ATM (2C1; GTX70103 [GeneTex, San Antonio, TX]), anti-ATR (GTX70133; GeneTex), anti-Chk2 (NT; ProSci, Poway, CA), anti-Chk2 (DCS-273; Medical and Biological Laboratories, Nagoya, Japan), anti-phospho-Chk2 (Thr68) (Cell Signaling,

Danvers, MA), anti-PARP-1 (C-2-10; Calbiochem, Merck Biosciences, Darmstadt, Germany), anti-hemagglutinin (HA) (HA-7; Sigma, St. Louis, MO), anti-core protein (CP-9 and CP-11; Institute of Immunology, Tokyo, Japan), anti-NS3 and anti-NS5B (no. 14; a generous gift from M. Kohara, the Tokyo Metropolitan Institute of Medical Science, Japan), anti-NS5A (no. 8926; a generous gift from A. Takamizawa, The Research Foundation for Microbial Diseases of Osaka University, Japan), and anti-β-actin (Sigma) Antibodies.

Immunofluorescence and confocal microscopic analysis. Cells were fixed in 3.5% formaldehyde in phosphate-buffered saline (PBS) and permeabilized in 0.1% NP-40 in PBS at room temperature. Cells were incubated with anti-ATM antibody (5C2; GTX70107 [GeneTex] or PM026 [MBL]), anti-HA antibody (3F10), anti-NS5B antibody and/or anti-NS3 antibody at a 1:300 dilution in PBS containing 3% bovine serum albumin at 37°C for 30 min. Cells were then stained with fluorescein isothiocyanate (FITC)-conjugated anti-rabbit antibody (Jackson ImmunoResearch, West Grove, PA) or anti-Cy3-conjugated anti-mouse antibody (Jackson ImmunoResearch) at a 1:300 dilution in PBS containing bovine serum albumin at 37°C for 30 min. Following extensive washing in PBS, cells were mounted on slides using a mounting medium of 90% glycerin–10% PBS with 0.01% *p*-phenylenediamine added to reduce fading. Samples were viewed under a confocal laser-scanning microscope (LSM510; Zeiss, Jena, Germany).

Immunoprecipitation. Cells were lysed in buffer containing 10 mM Tris-HCl (pH 8.0), 150 mM NaCl, 4 mM EDTA, 0.5% NP-40, 10 mM NaF, 1 mM dithiothreitol, and 1 mM phenylmethylsulfonyl fluoride. Lysates were precleared with 30 μl of protein G-Sepharose (GE Healthcare Biosciences, Uppsala, Sweden). Precleared supernatants were incubated with 5 μg of anti-HA antibody (3F10; Roche), 10 μl of anti-NS5B antibody, 5 μg of anti-Chk2 antibody (DCS-273; MBL), 5 μg of anti-FLAG antibody (M2; Sigma), or 5 μg of anti-ATM antibody (2C1) (GTX70103; GeneTex) at 4°C for 1 h. Following absorption of the precipitates on 30 μl of protein G-Sepharose resin for 1 h, the resin was washed four times with 700 μl of lysis buffer. Proteins were eluted by boiling the resin for 5 min in 2× Laemmli sample buffer. The proteins were then subjected to SDS-polyacrylamide gel electrophoresis, followed by immunoblotting analysis using anti-ATM, anti-Chk2, anti-HCV core protein (CP-9 and CP-11 mixture), anti-NS5A, anti-NS5B, anti-HA (HA-7; Sigma), or anti-NS3 antibody.

RESULTS

ATM and Chk2 are required for HCV RNA replication. To determine the potential role of DNA damage sensors in HCV replication, we first used lentiviral vector-mediated RNA interference to stably knockdown ATM, ATR, PARP-1 (1), or Chk2 in the following human hepatoma HuH-7-derived cell lines: O cells harboring a replicative genome-length HCV RNA (HCV-O, genotype 1b) (11), Oc cells derived from O cells (created by eliminating genome-length HCV RNA from O cells by IFN treatment) (11), sO cells harboring the subgenomic replicon of HCV-O (14), or RSc cells that cell culture-generated HCV (HCVcc) (JFH1, genotype 2a) (29) could infect and effectively replicate (3). To express shRNAs targeted to ATM, ATR, PARP-1 (1), or Chk2, we used a VSV-G-pseudotyped HIV-1-based vector system (24). We used puromycin-resistant pooled cells 10 days after the lentiviral transduction in all experiments. Western blot analysis of the lysates demonstrated very effective knockdown of ATM, ATR, Chk2, and PARP-1 in Oc cells (Fig. 1A). The effective knockdown of ATM, ATR, Chk2, or PARP-1 in O cells or sO cells was also confirmed by Western blot analysis (data not shown). In this context, the efficiency of colony formation (ECF) in ATM- or Chk2-, but not ATR- or PARP-1-, knockdown Oc cells transfected with the genome-length HCV-O RNA with an adapted mutation at amino acid position 1609 in the NS3 helicase region (ON/C-5B K1609E RNA) (11) was notably reduced compared with the control cells (Fig. 1B) even though Chk2-knockdown cells had a slightly faster growth rate than the control cells (Fig. 1C), suggesting that both ATM and Chk2 are crucial for HCV RNA replication. To further confirm this

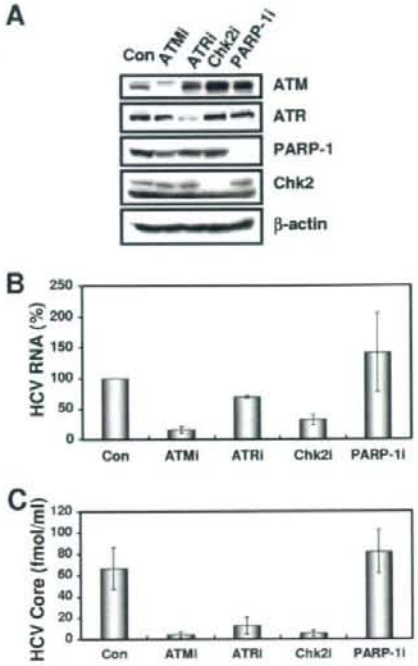

FIG. 2. ATM affects HCV infection. (A) Inhibition of ATM, ATR, Chk2, or PARP-1 expression by shRNA-producing lentiviral vectors. The results of Western blot analysis of cellular lysates with anti-ATM, anti-ATR, anti-PARP-1, anti-Chk2, or anti-β-actin antibody in RSc cured cells expressing shRNA targeted to ATM (ATMi), ATR (ATRi), Chk2 (Chk2i), or PARP-1 (PARP-1i) as well as in RSc cells transduced with a control lentiviral vector (Con) are shown. (B) The level of genome-length HCV (JFH1) RNA was monitored by real-time LightCycler PCR after inoculation of the HCVcc. Results from three independent experiments are shown as described in the legend of Fig. 1D. (C) The levels of the core protein in the culture supernatants were determined by enzyme-linked immunosorbent assay (Mitsubishi Kagaku Bio-Clinical Laboratories). Experiments were done in triplicate, and columns represent the mean core protein levels.

observation, we quantitatively examined the level of HCV RNA in the O cell- or sO cell-derived knockdown cells. Consequently, we found that replication of both genome-length HCV RNA (HCV-O) and its subgenomic replicon RNA (sO) were notably suppressed in ATM- or Chk2-knockdown cells but not in ATR- or PARP-1-knockdown cells (Fig. 1D and E). Consistent with this finding, the expression levels of core and NS5B proteins were also significantly decreased in the cell lysates of ATM- or Chk2-knockdown O cells (Fig. 1F). We next examined the replication level of HCV-JFH1 in ATM-, ATR-, Chk2-, or PARP-1-knockdown RSc cells (Fig. 2A). The results revealed that RNA replication of HCV-JFH1 and release of core protein into the culture supernatants were suppressed in only ATM- or Chk2-knockdown RSc cells after inoculation with HCVcc (Fig. 2B and C). Interestingly, the release of core protein into the culture supernatant was also significantly suppressed in ATR-knockdown RSc cells, while HCV RNA replication was slightly suppressed in these cells

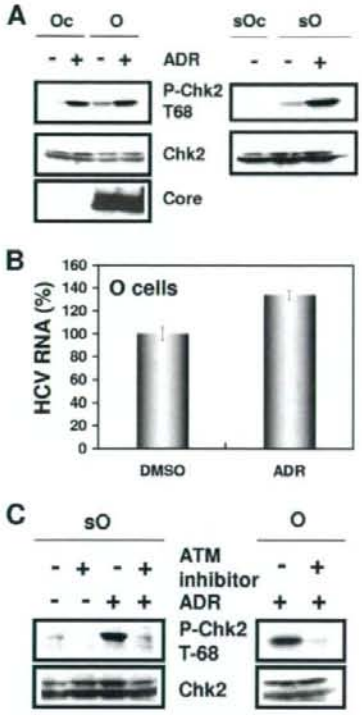

FIG. 3. ATM-dependent DNA damage response in HCV RNA-replicating cells. (A) Stimulation of Chk2 phosphorylation in the HCV RNA-replicating cells. The Oc, O, or sO cells were treated with 100 nM adriamycin (Sigma) for 2 h. The results of Western blot analysis of cellular lysates with anti-phospho-Chk2 (Thr68) (P-Chk2 T68), anti-Chk2, or anti-core protein antibody are shown. (B) Effect of adriamycin on HCV RNA replication. The O cells were treated with 100 nM adriamycin for 24 h. The level of genome-length HCV-O RNA was monitored by real-time LightCycler PCR. Results from three independent experiments are shown as described in the legend of Fig. 1D. DMSO, dimethyl sulfoxide. (C) Effect of ATM kinase inhibitor on Chk2 phosphorylation. The sO or O cells were pretreated with 10 μM ATM kinase inhibitor (KU-55933) (Calbiochem) for 2 h, followed by treatment with 100 nM adriamycin for 2 h. The results of Western blot analysis of cellular lysates with anti-phospho-Chk2 (Thr68) or anti-Chk2 antibody are shown.

(Fig. 2B and C), suggesting that ATR participates in the production of HCV virion.

In contrast, highly efficient knockdown of PARP-1 had no observable effects on the ECF (Fig. 1B), HCV RNA replication (Fig. 1D and E and 2B), or core protein expression in the cell lysate or in the supernatant (Fig. 1F and 2C), suggesting that our finding was not due to a nonspecific event. Thus, we have demonstrated for the first time that DNA damage sensors, ATM and Chk2, are required for HCV RNA replication.

ATM kinase activity in HCV RNA-replicating cells. Although it has been proposed that HCV causes dsDNA breaks (18, 19), little is known about whether HCV activates or inhibits the ATM-dependent damage response pathway. In this regard, it is worth noting that we observed weak but significant Chk2 phosphorylation at threonine 68, the specific marker for

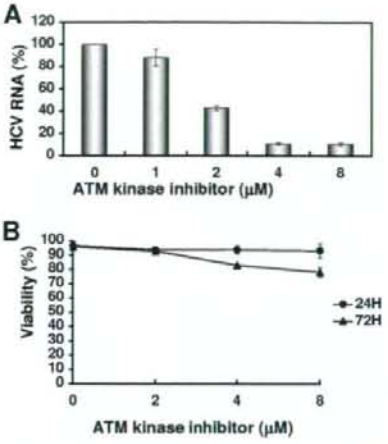

FIG. 4. Suppression of HCV RNA replication by ATM kinase inhibitor. (A) The level of genome-length HCV-O RNA was monitored by real-time LightCycler PCR after treatment with the indicated concentration of ATM kinase inhibitor for 72 h. Results from three independent experiments are shown as described in the legend of Fig. 1D. (B) Cell viabilities after treatment with the indicated concentration of ATM kinase inhibitor for 24 h or 72 h are shown.

ATM activation (20, 21), in the HCV RNA-replicating cells (O and sO cells) but not in the HCV-negative Oc and sOc cells (created by eliminating replicon RNA from sO cells by IFN treatment) (Fig. 3A), suggesting that the persistent HCV RNA replication stimulated the ATM-dependent DNA damage response. Furthermore, a 2-h treatment with 100 nM adriamycin, a dsDNA break inducer, markedly induced Chk2 phosphorylation in Oc, O, and sO cells (Fig. 3A). Importantly, Chk2 phosphorylation was not inhibited even in the HCV RNA-replicating cells (O and sO cells) (Fig. 3A), suggesting that the persistent HCV RNA replication and the HCV proteins are not able to suppress the ATM-dependent DNA damage response. To examine whether such a DNA damage response activates HCV RNA replication, we quantified the level of HCV RNA in the O cells treated with 100 nM adriamycin for 24 h. The results show that HCV RNA replication was increased (approximately 1.3-fold) after treatment with adriamycin (Fig. 3B), suggesting that the DNA damage response activates HCV RNA replication.

Suppression of HCV RNA replication by a small-molecule inhibitor of the ATM kinase. We next examined the effect of a specific small-molecule inhibitor of the ATM kinase (2-morpholin-4-yl-6-thianthren-1-yl-pyran-4-one [KU-55933]) (16) on HCV RNA replication. As expected, the ATM kinase inhibitor effectively inhibited Chk2 phosphorylation after adriamycin treatment in both sO and O cells (Fig. 3C). In this context, the ATM kinase inhibitor could efficiently suppress genome-length HCV RNA replication with an in vitro 50% effective concentration (EC_{50}) of approximately 2 μM at 72 h after treatment with adriamycin (Fig. 4A). Although this ATM kinase inhibitor did not affect cell viability at 24 h after the treatment, there was a slight decrease in the cell viability at 72 h after treatment (Fig. 4B). Thus, this or other ATM kinase inhibitors may be

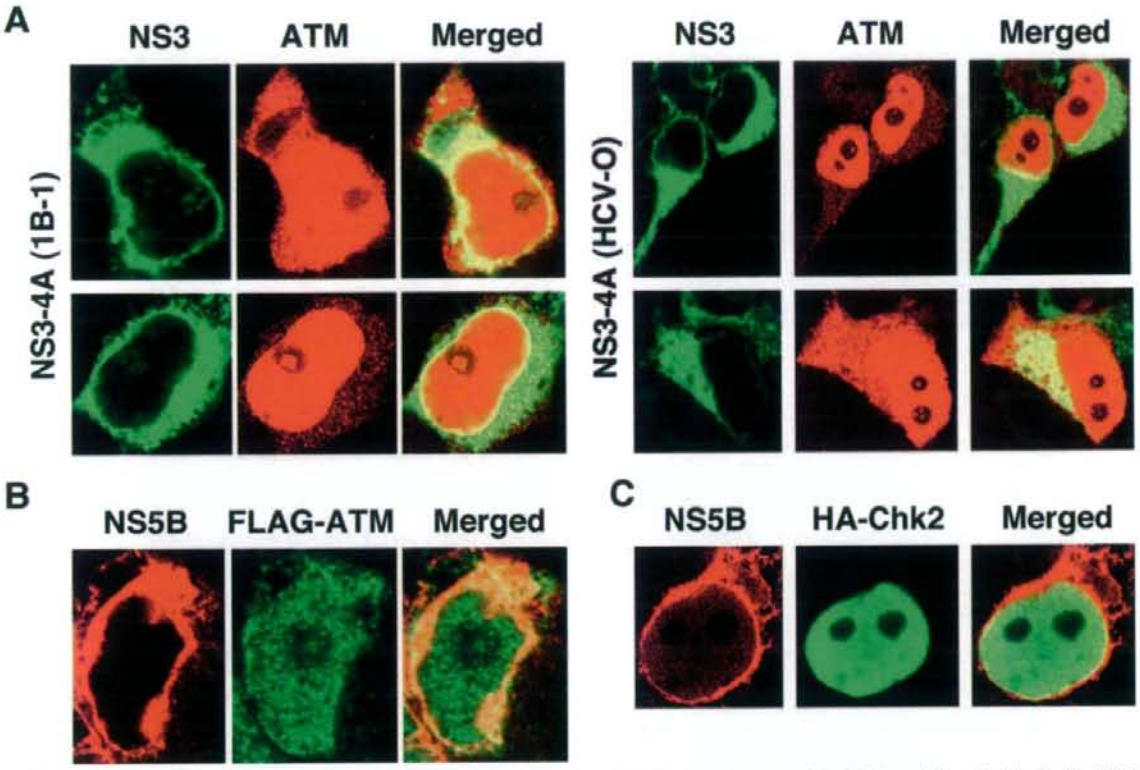

FIG. 5. Subcellular localization of ATM and Chk2 in HCV NS3-4A- or NS5B-expressing cells. (A) ATM partially colocalized with HCV NS3-4A. 293FT cells cotransfected with 300 ng of pCX4bsr/NS3-4A (1B-1) (8) or pCX4bsr/NS3-4A (O) (8) and 300 ng of pcDNA3-FLAG-ATMwt (6) were examined by confocal laser scanning microscopy. Cells were stained with anti-NS3 and anti-ATM (5C2) antibodies and then visualized with FITC (NS3) or Cy3 (ATM). (B) ATM partially colocalized with HCV NS5B. 293FT cells cotransfected with 300 ng of pCX4bsr/NS5B (1B-1) (23) and 300 ng of pcDNA3-FLAG-ATMwt (6). Cells were stained with anti-NS5B (no. 14) and anti-ATM (PM026) antibodies and then visualized with FITC (ATM) or Cy3 (NS5B). (C) Chk2 partially colocalized with HCV NS5B. 293FT cells cotransfected with 300 ng of pCX4bsr/NS5B (1B-1) (23) and 300 ng of pcDNA3-HA-Chk2wt (20, 21). Cells were stained with anti-NS5B and anti-HA (3F10) antibodies and then visualized with FITC (HA-Chk2) or Cy3 (NS5B). Images were visualized using confocal laser scanning microscopy (LSM510; Carl Zeiss). The right panels exhibit two-color overlay images (Merged). Colocalization is shown in yellow.

useful for the clinical treatment of patients with chronic hepatitis C.

Interaction of HCV NS3-4A with ATM. Since HCV NS3 has been proposed to be a viral factor involved in the induction of dsDNA breaks (18, 19), we first examined the subcellular localization of NS3-NS4A ([NS3-4A] 1B-1 or HCV-O strain) and ATM by confocal laser scanning microscopy. In most of the observed cells, ATM partially colocalized with NS3-4A in the perinuclear region and in dispersed points throughout the cytoplasm (Fig. 5A). In particular, we observed prominent colocalization of ATM with NS3-4A in some cells (Fig. 5A). Next, using anti-FLAG and anti-ATM antibodies, we immunoprecipitated lysates from 293FT cells in which FLAG-tagged ATM and either NS3-4A (HCV-O) or NS3 (HCV-O) were overexpressed and then performed immunoblotting analysis using either anti-ATM or anti-NS3 antibody to determine whether ATM binds to NS3-4A or NS3. The results revealed that ATM preferentially bound to NS3-4A over NS3 alone (Fig. 6A). Similarly, we found that ATM bound to NS3-4A using the O cell lysates (Fig. 6B), while HA-tagged Chk2 did not bind to NS3-4A in immunoprecipitation analysis using lysates from 293FT cells in which NS3-4A and HA-tagged Chk2 were overexpressed (Fig. 6C). Although NS3-4A has protease activity, ATM was not cleaved by the NS3-4A protease (Fig. 6D). Taking these results together, we conclude that ATM is able to interact with NS3-4A.

Interaction of HCV NS5B with ATM and Chk2. We next examined the subcellular localization of ATM and/or Chk2 in HCV NS5B-expressing cells by confocal laser scanning microscopy since we previously demonstrated that HCV NS5B-expressing PH5CH8 immortalized human hepatocyte cells were susceptible to DNA damage in the form of dsDNA breaks (23). ATM partially colocalized with NS5B in dispersed points throughout the cytoplasm (Fig. 5B), similar to the subcellular localization of HCV NS3-4A and ATM. Furthermore, Chk2 also partially colocalized with NS5B in the perinuclear region and in dispersed points in the nucleus (Fig. 5C). To determine whether endogenous ATM binds to NS5B, lysates from Oc or

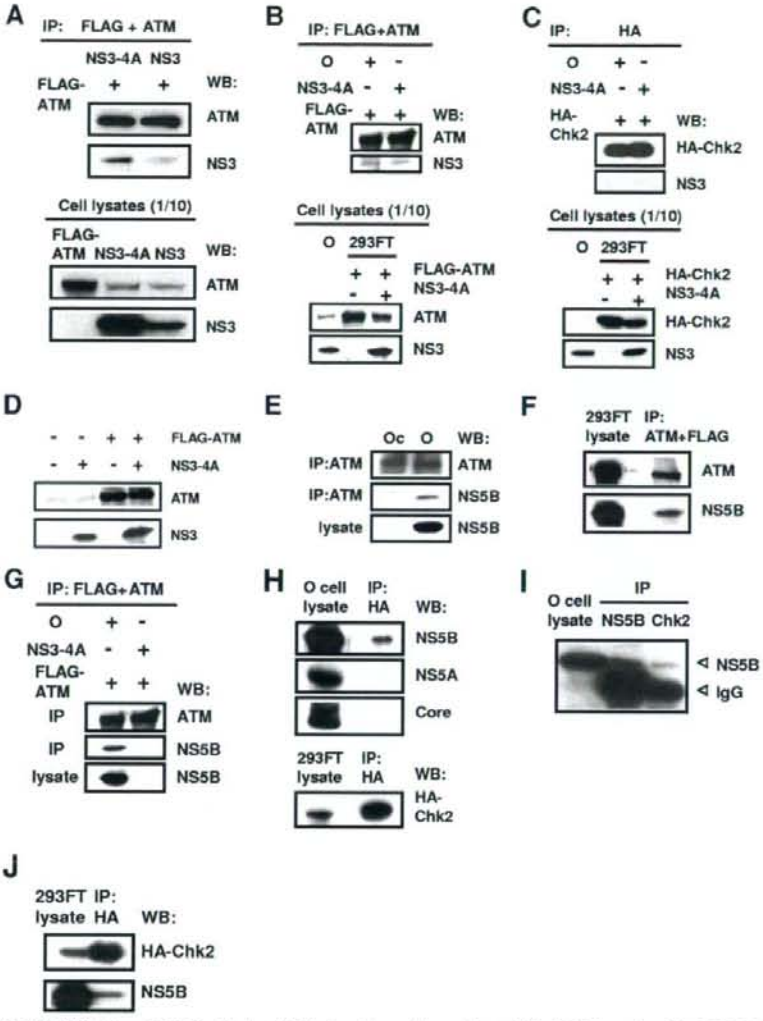

FIG. 6. Interaction of HCV NS3-4A and NS5B with the ATM signaling pathway. (A and B) ATM bound to HCV NS3-4A. (A) 293FT cells were transfected with 4 μg of pCX4bsr/NS3-4A (O), 4 μg of pCX4bsr/NS3 (O), or 4 μg of pcDNA3-FLAG-ATMwt. The cell lysates of expressed FLAG-ATM were mixed with lysates expressing either NS3-4A or NS3. The cell lysates were immunoprecipitated with both anti-FLAG (M2) and anti-ATM (2C1) antibodies, followed by immunoblotting analysis using either anti-ATM (2C1) or anti-HCV NS3 antibody. The results of Western blot analysis of 1/10 of the cellular lysates with anti-ATM or anti-NS3 antibody are also shown. (B) 293FT cells were cotransfected with 4 μg of pcDNA3-FLAG-ATMwt and/or 4 μg of pCX4bsr/NS3-4A (O). The cell lysates of expressed FLAG-ATM alone were mixed with the O cell lysates. Immunoprecipitation and Western blot analysis were performed as described in panel A. (C) Chk2 did not bind to NS3-4A. 293FT cells were cotransfected with 4 μg of pcDNA3-HA-Chk2wt and/or 4 μg of pCX4bsr/NS3-4A (O). The cell lysates of expressed HA-Chk2 alone were mixed with the O cell lysates. The cell lysates were immunoprecipitated with anti-HA antibody (3F10), followed by Western blot analysis using either anti-HA (HA-7) or anti-HCV NS3 antibody. The results of Western blot analysis of 1/10 of the cellular lysates with anti-HA or anti-NS3 antibody are also shown. (D) ATM was not cleaved by HCV NS3-4A protease. 293FT cells were cotransfected with 4 μg of pCX4bsr/NS3-4A (O) and/or 4 μg of pcDNA3-FLAG-ATMwt. The results of Western blot analysis of cellular lysates with anti-ATM or anti-NS3 antibody are shown. (E to G) ATM bound to HCV NS5B. (E) The lysates of O or Oc cells were immunoprecipitated with anti-ATM antibody (2C1), followed by immunoblotting analysis using either anti-ATM or anti-HCV NS5B antibody (no. 14). The results of Western blot analysis of 1/10 of the cellular lysates with anti-NS5B antibody are also shown. (F) 293FT cells were cotransfected with 4 μg of pCX4bsr/NS5B (1B-1) and 4 μg of pcDNA3-FLAG-ATMwt. The cell lysates were immunoprecipitated with both anti-FLAG and anti-ATM antibodies, followed by immunoblotting analysis using either anti-ATM or anti-HCV NS5B antibody. (G) Western Blot analysis was performed with anti-NS5B antibody, reusing the same blotted membrane that was used for panel B. (H to J) Chk2 bound to HCV NS5B. (H) 293FT cells were cotransfected with 4 μg of pcDNA3-HA-Chk2wt. The cell lysates of expressed HA-Chk2 were mixed with the O cell lysates and were immunoprecipitated with anti-HA antibody (3F10), followed by immunoblotting analysis using anti-HCV NS5B, anti-HCV NS5A (no. 8926), anti-HCV core protein (CP-9 and CP-11 mixture), or anti-HA (HA-7) antibody. The results of Western blot analysis of 1/10 of the cellular lysates with the same antibodies are also shown. (I) The lysates of O cells were immunoprecipitated with anti-NS5B or anti-Chk2 antibody (DCS-273), followed by immunoblotting analysis using anti-HCV NS5B antibody. The result of Western blot analysis of 1/10 of the cellular lysates with anti-NS5B antibody is also shown. (J) 293FT cells were cotransfected with 4 μg of pCX4bsr/NS5B (1B-1) and 4 μg of pcDNA3-HA-Chk2wt. The cell lysates were immunoprecipitated with anti-HA antibody (3F10), followed by immunoblotting analysis using either anti-HA (HA-7) or anti-HCV NS5B antibody. IP, immunoprecipitation; WB, Western blotting; IgG, immunoglobulin G.

O cells were immunoprecipitated with anti-ATM antibody, and then immunoblotting analysis using either anti-ATM or anti-NS5B antibody was performed. The results revealed that endogenous ATM bound to endogenous NS5B (Fig. 6E). Furthermore, we confirmed that ATM bound to NS5B in immunoprecipitation analysis using lysates from 293FT cells, in which NS5B (1B-1 strain) and FLAG-tagged ATM were overexpressed (Fig. 6F). Similarly, we confirmed that FLAG-tagged ATM bound to NS5B derived from O cell lysates in immunoprecipitation analysis using lysates from 293FT cells in which FLAG-tagged ATM was overexpressed (Fig. 6G). Finally, to determine which HCV protein binds to Chk2, the 293FT cell lysates of overexpressed HA-Chk2 were mixed with the O cell lysates and were immunoprecipitated with anti-HA antibody, followed by Western blot analysis using anti-HCV NS5B, anti-HCV NS5A, anti-HCV core protein, or anti-HA antibody. Consistent with the immunofluorescence result that Chk2 partially colocalized with NS5B (Fig. 5C), we observed that HA-tagged Chk2 bound to NS5B (Fig. 6H). Importantly, we found that endogenous Chk2 bound to endogenous NS5B derived from O cells (Fig. 6I). In addition, HA-tagged Chk2 bound to NS5B in immunoprecipitation analysis using lysates from 293FT cells in which NS5B (1B-1 strain) and HA-tagged Chk2 were overexpressed (Fig. 6J). Thus, Chk2 also interacted with NS5B as well as ATM. Taking these results together, we conclude that HCV targets ATM and Chk2 DNA damage sensors and that the ATM signaling pathway is required for HCV RNA replication.

DISCUSSION

ATM has been implicated as a target of most DNA viruses, harboring their genomes in the form of dsDNA which can activate or inhibit the ATM signaling pathway (17). In this study, we have demonstrated for the first time that the ATM signaling pathway is required for HCV RNA replication even though HCV does not have a dsDNA genome, unlike DNA viruses. In this regard, Machida et al. previously proposed that HCV infection and the expression of HCV NS3 and core protein induced dsDNA breaks (18, 19). Furthermore, NS3 has DNA helicase activity by which it unwinds dsDNA, suggesting that NS3 affects host dsDNA (22, 25). Thus, HCV infection might trigger the activation of ATM without a dsDNA genome. In fact, we observed weak but significant phosphorylation of Chk2 at threonine 68, the specific marker for ATM activation, in the HCV RNA-replicating cells (O and sO cells) but not in the HCV-negative Oc and sOc cells (Fig. 3A), suggesting that the ATM-dependent DNA damage response is constantly stimulated in persistent HCV RNA-replicating cells. Furthermore, we demonstrated that ATM preferentially bound to NS3-4A over NS3 alone (Fig. 5B) and that ATM partially colocalized with NS3-4A in the perinuclear region, where HCV is known to form a replication complex and replicate itself, and in dispersed points throughout the cytoplasm (Fig. 5A), indicating the interaction of ATM with NS3-4A. Interestingly, Lai et al. very recently reported that NS3-4A impaired DNA repair and enhanced sensitivity to ionizing radiation through interaction with ATM (15). However, we observed an equivalent level of Chk2 phosphorylation at threonine 68, a direct downstream target of ATM (20, 21), in both HCV RNA-replicating cells (O cells) and HCV-negative cells (Oc cells) after treatment with adriamycin (Fig. 3A), suggesting that Chk2 phosphorylation by ATM is not impaired by HCV RNA replication. In this regard, Gaspar and Shenk also showed that human cytomegalovirus could inhibit a DNA damage response by mislocalizing ATM and phosphorylated Chk2 at threonine 68 to a cytoplasmic virus assembly zone, indicating that human cytomegalovirus blocked at the level of Chk2 (9). On the other hand, dsDNA triggers IFN immune defenses through retinoic acid-induced gene I, the mitochondrial antiviral signaling protein, or the DNA-dependent activator of IFN-regulatory factor (7, 26); and NS3-4A protease, which is known to cleave the mitochondrial antiviral signaling protein, can block it (26), suggesting that interaction of NS3-4A with ATM is partially involved in such a common antiviral signaling pathway. On the other hand, we previously demonstrated that HCV NS5B-expressing PH5CH8 immortalized human hepatocyte cells were susceptible to DNA damage in the form of dsDNA breaks (23). In this regard, we have found that HCV NS5B could bind to both ATM and Chk2 (Fig. 5B and C and 6E to J). Together, these results indicate that HCV might hijack ATM and Chk2 and utilize ATM and Chk2 for HCV RNA replication, thereby resulting in impairment of DNA repair, enhancement of mutation frequency, and development of hepatocellular carcinoma.

Finally, consistent with our finding that ATM was required for HCV RNA replication, an ATM kinase inhibitor efficiently suppressed genome-length HCV RNA replication at an EC_{50} of approximately 2 μM at 72 h after the treatment (Fig. 4A). Similarly, Lau et al. reported that the same ATM kinase inhibitor could suppress HIV-1 replication at an EC_{50} of approximately 2.3 μM (16). Importantly, the EC_{50} for HIV-1 replication is similar to that for HCV replication. Thus, this or other ATM kinase inhibitors may represent a novel approach for the clinical treatment of patients with chronic hepatitis C as well as AIDS patients.

ACKNOWLEDGMENTS

We thank D. Trono, R. Agami, R. Iggo, M. Kastan, S. J. Elledge, M. Kohara, A. Takamizawa, and M. Hijikata for the VSV-G-pseudotyped HIV-1-based vector system (pCMVR8.91 and pMDG2) and for pSUPER, pRDI292, pcDNA3-FLAG-ATM, and pcDNA3-HA-Chk2, and for anti-NS3 antibody, anti-NS5B antibody, anti-NS5A antibody, and 293FT cells. We also thank A. Morishita and T. Nakamura for their technical assistance.

This work was supported by a Grant-in-Aid for Young Scientists (B) from the Ministry of Education, Culture, Sports, Science and Technology (MEXT); by a Grant-in-Aid for Research on Hepatitis from the Ministry of Health, Labor, and Welfare of Japan; by the Ichiro Kanehara Foundation; and by a Research Fellowship from the Japan Society for the Promotion of Science.

REFERENCES

1. **Ariumi, Y., P. Turelli, M. Masutani, and D. Trono.** 2005. DNA damage sensors ATM, ATR, DNA-PKcs, and PARP-1 are dispensable for human immunodeficiency virus type 1 integration. J. Virol. **79:**2973–2978.
2. **Ariumi, Y., and D. Trono.** 2006. Ataxia-telangiectasia-mutated (ATM) protein can enhance human immunodeficiency virus type 1 replication by stimulating Rev. function. J. Virol. **80:**2445–2452.
3. **Ariumi, Y., M. Kuroki, K. Abe, H. Dansako, M. Ikeda, T. Wakita, and N. Kato.** 2007. DDX3 DEAD-box RNA helicase is required for hepatitis C virus RNA replication. J. Virol. **81:**13922–13926.
4. **Bridge, A. J., S. Pebernard, A. Ducraux, A.-L. Nicoulaz, and R. Iggo.** 2003. Induction of an interferon response by RNAi vectors in mammalian cells. Nat. Genet. **34:**263–264.

5. **Brummelkamp, T. R., R. Bernard, and R. Agami.** 2002. A system for stable expression of short interfering RNAs in mammalian cells. Science **296:**550–553.
6. **Canman, C. E., D.-S. Lim, K. A. Cimprich, Y. Taya, K. Tamai, K. Sakaguchi, E. Apella, M. B. Kastan, and J. D. Siliciano.** 1998. Activation of the ATM kinase by ionizing radiation and phosphorylation of p53. Science **281:**1677–1679.
7. **Cheng, G., J. Zhong, J. Chung, and F. V. Chisari.** 2007. Double-stranded DNA and double-stranded RNA induces a common antiviral signaling pathway in human cells. Proc. Natl. Acad. Sci. USA **104:**9035–9040.
8. **Dansako, H., M. Ikeda, and N. Kato.** 2007. Limited suppression of the interferon-beta production by hepatitis C virus serine protease in cultured human hepatocytes. FEBS J. **274:**4161–4176.
9. **Gaspar, M., and T. Shenk.** 2006. Human cytomegalovirus inhibits a DNA damage response by mislocalizing checkpoint proteins. Proc. Natl. Acad. Sci. USA **103:**2821–2826.
10. **Harper, J. W., and S. J. Elledge.** 2007. The DNA damage response: ten years after. Mol. Cell **28:**739–745.
11. **Ikeda, M., K. Abe, H. Dansako, T. Nakamura, K. Naka, and N. Kato.** 2005. Efficient replication of a full-length hepatitis C virus genome, strain O, in cell culture, and development of a luciferase reporter system. Biochem. Biophys. Res. Commun. **329:**1350–1359.
12. **Kato, N., M. Hijikata, Y. Ootsuyama, M. Nakagawa, S. Ohkoshi, T. Sugimura, and K. Shimotohno.** 1990. Molecular cloning of the human hepatitis C virus genome from Japanese patients with non-A, non-B hepatitis. Proc. Natl. Acad. Sci. USA **87:**9524–9528.
13. **Kato, N.** 2001. Molecular virology of hepatitis C virus. Acta Med. Okayama **55:**133–159.
14. **Kato, N., K. Sugiyama, K. Namba, H. Dansako, T. Nakamura, M. Takami, K. Naka, A. Nozaki, and K. Shimotohno.** 2003. Establishment of a hepatitis C virus subgenomic replicon derived from human hepatocytes infected in vitro. Biochem. Biophys. Res. Commun. **306:**756–766.
15. **Lai, C. K., K. S. Jeng, K. Machida, Y. S. Cheng, and M. M. Lai.** 2008. Hepatitis C virus NS3/4A protein interacts with ATM, impairs DNA repair and enhances sensitivity to ionizing radiation. Virology **370:**295–309.
16. **Lau, A., K. M. Swinbank, P. S. Ahmed, D. L. Taylor, S. P. Jackson, G. C. Smith, and M. J. O'Connor.** 2005. Suppression of HIV-1 infection by a small molecule inhibitor of the ATM kinase. Nat. Cell Biol. **7:**493–500.
17. **Lilley, C. E., R. A. Schwartz, and M. D. Weitzman.** 2007. Using or abusing: viruses and the cellular DNA damage response. Trends Microbiol. **15:**119–126.
18. **Machida, K., K. T. Cheng, V. M. Sung, S. Shimodaira, K. L. Lindsay, A. M. Levine, M. Y. Lai, and M. M. Lai.** 2004. Hepatitis C virus induces a mutator phenotype: enhanced mutations of immunoglobulin and protooncogenes. Proc. Natl. Acad. Sci. USA **101:**4262–4267.
19. **Machida, K., K. T. Cheng, V. M. Sung, K. J. Lee, A. M. Levine, and M. M. Lai.** 2004. Hepatitis C virus infection activates the immunologic (type II) isoform of nitric oxide synthase and thereby enhances DNA damage and mutations of cellular genes. J. Virol. **78:**8835–8843.
20. **Matsuoka, S., M. Huang, and S. J. Elledge.** 1998. Linkage of ATM to cell cycle regulation by the Chk2 protein kinase. Science **282:**1893–1897.
21. **Matsuoka, S., G. Rotman, A. Ogawa, Y. Shiloh, K. Tamai, and S. J. Elledge.** 2000. Ataxia telangiectasia-mutated phosphorylates Chk2 in vivo and in vitro. Proc. Natl. Acad. Sci. USA **97:**10389–10394.
22. **Myong, S., M. M. Bruno, A. M. Pyle, and T. Ha.** 2007. Spring-loaded mechanism of DNA unwinding by hepatitis C virus NS3 helicase. Science **317:**513–516.
23. **Naka, K., H. Dansako, N. Kobayashi, M. Ikeda, and N. Kato.** 2006. Hepatitis C virus NS5B delays cell cycle progression by inducing interferon-β via Toll-like receptor 3 signaling pathway without replicating viral genomes. Virology **346:**348–362.
24. **Naldini, L., U. Blömer, P. Gallay, D. Ory, R. Mulligan, F. H. Gage, I. M. Verma, and D. Trono.** 1996. In vivo gene delivery and stable transduction of nondividing cells by a lentiviral vector. Science **272:**263–267.
25. **Pang, P. S., E. Jankowsky, P. J. Planet, and A. M. Pyle.** 2002. The hepatitis C viral NS3 protein is a processive DNA helicase with cofactor enhanced RNA unwinding. EMBO J. **21:**1168–1176.
26. **Takaoka, A., Z. Wang, M. K. Choi, H. Yanai, H. Negishi, T. Ban, Y. Lu, M. Miyagishi, T. Kodama, K. Honda, Y. Ohba, and T. Taniguchi.** 2007. DAI (DLM-1/ZBP1) is a cytosolic DNA sensor and an activator of innate immune response. Nature **448:**501–505.
27. **Tanaka, T., N. Kato, M. J. Cho, and K. Shimotohno.** 1995. A novel sequence found at the 3′ terminus of hepatitis C virus genome. Biochem. Biophys. Res. Commun. **215:**744–749.
28. **Thomas, D. L.** 2000. Hepatitis C epidemiology. Curr. Top. Microbiol. Immunol. **242:**25–41.
29. **Wakita, T., T. Pietschmann, T. Kato, T. Date, M. Miyamoto, Z. Zhao, K. Murthy, A. Habermann, H. G. Kräusslich, M. Mizokami, R. Bartenschlager, and T. J. Liang.** 2005. Production of infectious hepatitis C virus in tissue culture from a cloned viral genome. Nat. Med. **11:**791–796.
30. **Zufferey, R., D. Nagy, R. J. Mandel, L. Naldini, and D. Trono.** 1997. Multiply attenuated lentiviral vector achieves efficient gene delivery in vivo. Nat. Biotechnol. **15:**871–875.

Virus Research 137 (2008) 72–79

Contents lists available at ScienceDirect

Virus Research

journal homepage: www.elsevier.com/locate/virusres

A new living cell-based assay system for monitoring genome-length hepatitis C virus RNA replication

Hiromichi Dansako, Masanori Ikeda, Ken-ichi Abe, Kyoko Mori, Kazunori Takemoto, Yasuo Ariumi, Nobuyuki Kato*

Department of Molecular Biology, Okayama University Graduate School of Medicine, Dentistry, and Pharmaceutical Sciences, 2-5-1 Shikata-cho, Okayama 700-8558, Japan

ARTICLE INFO

Article history:
Received 22 February 2008
Received in revised form 6 June 2008
Accepted 6 June 2008
Available online 21 July 2008

Keywords:
Hepatitis C virus
Genome-length HCV RNA
Living cell-based assay
Green fluorescent protein
OGF7 assay system
Anti-HCV reagents

ABSTRACT

We previously developed a cell-based luciferase reporter assay system for monitoring genome-length hepatitis C virus (HCV) RNA replication (OR6 assay system). Here, we aimed to develop a new living cell-based reporter assay system using enhanced green fluorescent protein (EGFP). Genome-length HCV RNAs encoding EGFP were introduced into a subline of HuH-7 cells and G418 selection was performed. One cloned cell line, OGF7, was successfully selected from among the several G418-resistant cell lines obtained, and the robust expression of HCV RNA and proteins in OGF7 cells was confirmed. The fluorescent intensity of OGF7 cells was decreased by interferon-α treatment in a dose-dependent manner, and it correlated well with the HCV RNA concentration. We demonstrated that the interferon-α sensitivity in the OGF7 assay system measuring the fluorescent intensity was equivalent to that of the OR6 assay system, and that the OGF7 assay system was useful for quantitative evaluation of anti-HCV reagents. The OGF7 assay system is expected to be the most time-saving and inexpensive assay system for high-throughput screening of anti-HCV reagents.

1. Introduction

Persistent hepatitis C virus (HCV) infection frequently causes active liver disease in the form of chronic hepatitis (Choo et al., 1989; Kuo et al., 1989), liver cirrhosis, and hepatocellular carcinoma (Ohkoshi et al., 1990; Saito et al., 1990). HCV infection has now become a serious health problem, with at least 170 million people currently infected worldwide (Thomas, 2000). HCV is an enveloped positive single-stranded RNA (9.6 kb) virus belonging to the *Flaviviridae* (Kato et al., 1990; Tanaka et al., 1995). The HCV genome encodes a large polyprotein precursor of approximately 3000 amino acid (aa) residues, which is cleaved co- and post-translationally into at least 10 proteins in the following order: core, envelope 1 (E1), E2, p7, non-structural protein 2 (NS2), NS3, NS4A, NS4B, NS5A, and NS5B. These cleavages are mediated by the host and virally encoded proteases (Hijikata et al., 1991, 1993; Kato, 2001). NS5B possessing an RNA-dependent RNA polymerase (RdRp) activity is the central enzyme in replication of the HCV genome (Kato, 2001).

In the recent past, interferon (IFN) was used as the main treatment for patients with chronic hepatitis C. Currently, the combination of pegylated-IFN (PEG-IFN) and ribavirin is the standard therapy worldwide, although only 50% of patients show a sustained virological response to this therapy (Hayashi and Takehara, 2006). Several clinical drugs have been proposed as adjuvants to IFN, including cyclosporine A (CsA) (Watashi et al., 2003), mizoribine (Naka et al., 2005), and statins (Ikeda et al., 2006; Ye et al., 2003). Currently, NS3 proteinase/helicase activity and NS5B RdRp activity have been considered as targets for the development of anti-HCV reagents (e.g., the NS3 protease inhibitor BILN 2061 (Lamarre et al., 2003). To date, however, we have not obtained HCV-specific drugs possessing more effective anti-HCV activity than PEG-IFN. Therefore, a more convenient high-throughput screening system is still required to explore more effective anti-HCV reagents.

We previously developed a cell-based genome-length HCV RNA replication system using *Renilla* luciferase as a reporter in order to monitor the HCV RNA replication level (OR6 assay system) (Ikeda et al., 2005; Naka et al., 2005). Other groups have also developed cell-based subgenomic HCV replicon systems using secreted alkaline phosphatase (Yi et al., 2002) or beta-lactamase (Murray et al., 2003) as a reporter. However, these assay systems are still quite time- and cost-intensive methods for measuring enzyme activity.

In the present study, we report a new living cell-based reporter assay system that is able to monitor the level of genome-length HCV RNA replication and to reduce both the time required and the expense.

* Corresponding author. Tel.: +81 86 235 7385; fax: +81 86 235 7392.
E-mail address: nkato@md.okayama-u.ac.jp (N. Kato).

0168-1702/$ – see front matter © 2008 Elsevier B.V. All rights reserved.
doi:10.1016/j.virusres.2008.06.001

2. Materials and methods

2.1. Reagents

IFN-α, IFN-γ, and CsA were purchased from Sigma–Aldrich (St. Louis, MO). IFN-β was a gift from Toray Industries (Tokyo, Japan). Fluvastatin (FLV) was purchased from Calbiochem (San Diego, CA).

2.2. Cell culture

Genome-length HCV RNA replicating cells and OR6c cells were maintained as described previously (Ikeda et al., 2005). OR6c cells are cured OR6 cells (Naka et al., 2005) from which genome-length HCV RNA was eliminated by IFN-α treatment as described previously (Ikeda et al., 2005).

2.3. Construction of plasmids and RNA synthesis

The plasmids used in this study (Fig. 1A and B) were constructed on the basis of the plasmid pON/C-5B/KE (Ikeda et al., 2005). The plasmid pON/C-5B/KE contains neomycin phosphotransferase (Neo^R) downstream of HCV internal ribosome entry site (IRES) and the full-length HCV-O polyprotein-coding sequence downstream of the encephalomyocarditis virus (EMCV) IRES, and K1609E mutation (Ikeda et al., 2005), was introduced into the NS3 helicase region as the adaptive mutation. The plasmid pOGN/C-5B/KE (Fig. 1A(1)) was constructed from the plasmid pON/C-5B/KE by inserting the PCR product of enhanced green fluorescent protein (EGFP; Clontech Laboratories, Inc., Mountain View, CA) into the AscI recognition site of the 5′-end of the Neo^R gene. The plasmids pON/GC-5B/KE (Fig. 1A(2)) and pON/C-5B G2390/KE (Fig. 1A(3)) were constructed from the plasmid pON/C-5B/KE by inserting the PCR product of EGFP into the XhoI recognition site of the 5′-end of the core-coding sequence and at aa position 2390 (Moradpour et al., 2004) in the NS5A-coding sequence, respectively. Both recognition sites were introduced by PCR mutagenesis with primers containing these recognition sites according to the previously described method (Dansako et al., 2005). To construct the plasmids pOGN/C-5B G2390/KE (Fig. 1B(4)) and pON/GC-5B G2390/KE (Fig. 1B(6)), the EcoRI-SpeI fragments of the plasmids pOGN/C-5B/KE and pON/GC-5B/KE, respectively, were replaced with the EcoRI-SpeI region of the plasmid pON/C-5B G2390/KE. The EcoRI recognition site is located at the 5′-end of HCV IRES, and the SpeI recognition site is located at the 5′-end of the NS3 region within the plasmid pON/C-5B/KE, respectively. To construct the plasmids pOGN/GC-5B/KE (Fig. 1B(5)) and pOGN/GC-5B G2390/KE (Fig. 1B(7)), the EcoRI-RsrII fragment of the plasmid pOGN/C-5B/KE was replaced with the EcoRI-RsrII region of the plasmids pON/GC-5B/KE and pON/GC-5B G2390/KE, respectively. The RsrII recognition site is located in the 3′-end of the Neo^R region within the plasmid pON/C-5B/KE. The obtained plasmids were linearized by XbaI and were used for RNA synthesis with T7 MEGAscript (Ambion, Austin, TX) as previously described (Kato et al., 2003).

2.4. RNA transfection and selection of G418-resistant cells

The transfection of genome-length HCV RNA synthesized in vitro into OR6c cells was performed by electroporation, and the cells were selected in the presence of G418 (0.3 mg/ml; Invitrogen) for 3 weeks as described previously (Kato et al., 2003).

2.5. Visualization of the fluorescence by EGFP

The fluorescence of EGFP was directly visualized by a fluorescence microscope (Axiovert 25CFL; Carl Zeiss) or a confocal laser-scanning microscope (LSM510; Carl Zeiss). The cells were fixed with 4% paraformaldehyde and were photographed under a fluorescence microscope or a confocal laser-scanning microscope as described previously (Dansako et al., 2003).

2.6. Integration analysis

Genomic DNA was extracted from the cultured cells by using a DNeasy Blood & Tissue Kit (QIAGEN, Valencia, CA). The HCV 5′-untranslated region (UTR) and the IFN-β gene were detected according to a method described previously (Kato et al., 2003). To test the efficiency of the PCR analysis and the quality of the genomic DNAs, a set of primers was used for the PCR detection of an intronless IFN-β gene (1 copy per haploid genome; the expected PCR product is 341 bp).

2.7. Northern blot analysis

Total RNA was extracted from the cultured cells by using an RNeasy Mini Kit (QIAGEN). HCV RNA and β-actin were detected according to a method described previously (Ikeda et al., 2005).

2.8. Measurement of the fluorescent intensity in living cells replicating a genome-length HCV RNA with EGFP

The cells replicating a genome-length HCV RNA with EGFP (5×10^4) were plated onto 12-well plates. By using a fluorometer (Fluoroskan Ascent; Thermo Fisher Scientific K.K., Yokohama, Japan), the fluorescent intensity in living cells was measured at 24, 48, and 72 h. In several experiments, the fluorescent intensity in living cells was measured only at 72 h after the treatment with reagents. After the measurements of the fluorescent intensity, the cells were subjected to Western blot analysis for HCV proteins and quantitative RT-PCR analysis for HCV RNA.

2.9. Western blot analysis

The preparation of cell lysates, the sodium dodecyl sulfate-polyacrylamide gel electrophoresis, and the immunoblotting analysis were performed as previously described (Hijikata et al., 1993). Production of core, E1, NS3, NS5A, and NS5B proteins in the O and OGF7 cells was analyzed by immunoblotting using anti-core (CP11; Institute of Immunology, Tokyo, Japan), anti-E1 (a generous gift from Dr. M. Kohara, Tokyo Metropolitan Institute of Medical Science), anti-NS3 (Novocastra Laboratories, Newcastle, UK), anti-NS5A (a generous gift from Dr. A. Takamizawa, Research Foundation for Microbial Diseases, Osaka University), and anti-NS5B (a generous gift from Dr. M. Kohara, Tokyo Metropolitan Institute of Medical Science) antibodies, respectively. Production of EGFP-Neo^R fusion protein was also detected by anti-GFP antibody (JL-8; Clontech). β-Actin antibody (AC-15; Sigma) was used as the control for the amount of protein loaded per lane. Immunocomplexes were detected with the Renaissance enhanced chemiluminescence assay (PerkinElmer Life Sciences, Boston, MA).

2.10. Quantitative RT-PCR analysis

The quantitative RT-PCR analysis for HCV RNA was performed by using a real-time LightCycler PCR as described previously (Ikeda et al., 2005).

3. Results

3.1. Establishment of the cloned cell lines replicating a genome-length HCV RNA with EGFP

We previously developed a dicistronic genome-length HCV RNA (O strain of genotype 1b) replication system that stably expresses *Renilla* luciferase as a reporter in order to monitor the level of HCV RNA replication (OR6 assay system) (Ikeda et al., 2005; Naka et al., 2005). To further facilitate mass screening of potential candidates for anti-HCV reagents, we attempted to develop a novel assay system for monitoring the level of HCV RNA replication without lysis of cells. For this purpose, we chose EGFP as a reporter, and we first tried to establish cloned cell lines that efficiently replicate genome-length HCV RNA encoding EGFP. All of the constructed plasmids (Fig. 1) were used as templates for RNA synthesis in vitro, and then the transcribed RNAs were transfected into OR6c cells by the electroporation method, as described in Section 2. After 3 weeks of G418 selection, we obtained several G418-resistant colonies from the OGN/C-5B/KE RNA, ON/GC-5B/KE RNA, ON/C-5B G2390/KE RNA, or OGN/GC-5B/KE RNA-introduced cells, and most of the G418-resistant colonies were successfully established as cell lines (Fig. 1). In contrast, no G418-resistant colonies were obtained from the OGN/C-5B G2390/KE RNA, ON/GC-5B G2390/KE RNA, or OGN/GC-5B G2390/KE RNA-introduced cells (Fig. 1).

To select a cloned cell line showing the highest expression level of EGFP and HCV protein, we first performed Western blot analysis for the detection of EGFP and HCV NS3 protein. The results revealed that OGN/C-5B/KE clone 7, ON/GC-5B/KE clone 3, and OGN/GC-5B/KE clone 3 showed marginally higher expression levels of EGFP and HCV NS3 protein than the other clones (data not shown). Because, in the examination by fluorescence microscopy,

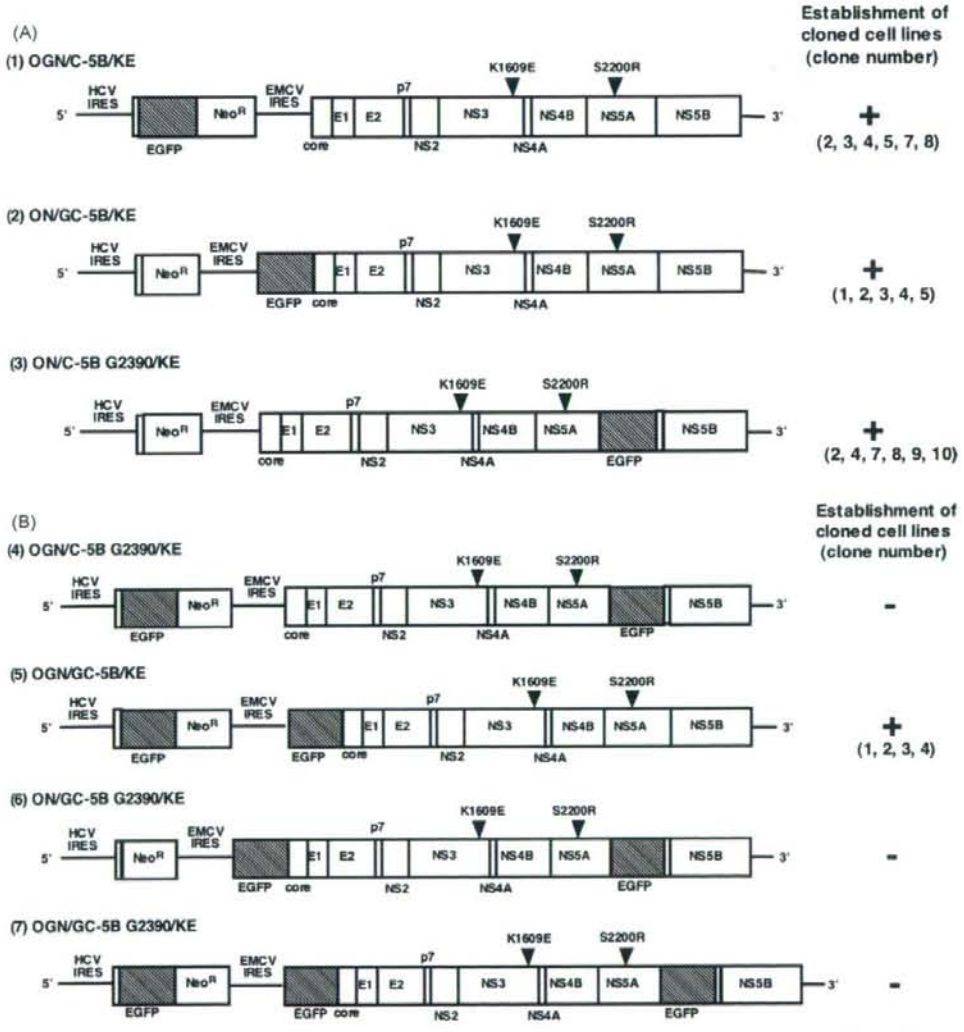

Fig. 1. Schematic presentation of various genome-length HCV RNAs (HCV-O strain) containing an EGFP-encoding sequence. (A) Genome-length HCV RNAs containing one copy of the EGFP-encoding sequence. The basic construct is described in our previous study (Ikeda et al., 2005). The EGFP-encoding region is depicted as a shaded box. Neomycin phosphotransferase is indicated as Neo^R. K1609E and S2200R are adaptive mutations found in previous studies (Ikeda et al., 2005; Kato et al., 2003). (B) Genome-length HCV RNAs containing two or three copies of EGFP-encoding sequence.

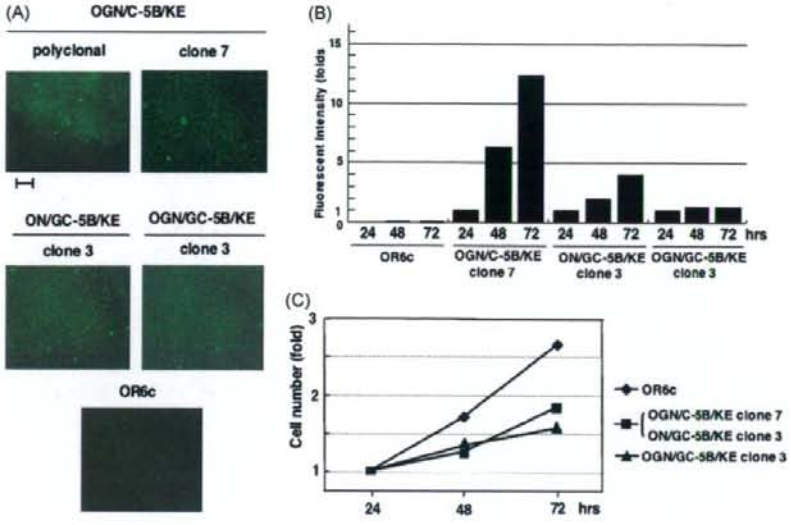

Fig. 2. Fluorescent intensities of G418-resistant cell lines. (A) Visualization of the fluorescence of G418-resistant cell lines under a fluorescence microscope. The panels show the fluorescence of expressed EGFP. Bar, 200 μm. (B) Time course of the fluorescent intensity of G418-resistant cell lines. The fluorescent intensity was measured at 24, 48, and 72 h after cell-seeding by a fluorometer as described in Section 2. For calculating the fluorescent intensity in each cell line, the intensity at 24 h after cell seeding was assigned a value of 1. OR6c cells were used as a negative control. (C) Growth curve of G418-resistant cell lines. The cells were plated onto 6-well plate (1×10^5 cells per well), and the kinetics of cell proliferation during 72 h in culture were determined by Trypan blue treatment. OR6c cells were used as a control.

the fluorescence of EGFP in these selected cell lines was roughly equivalent to that in OGN/C-5B/KE polyclonal cells (Fig. 2A), we next examined the time course of the fluorescent intensities of these cells lines by using a fluorometer, and observed a remarkable, twelve-fold increase in the fluorescent intensity of OGN/C-5B/KE clone 7 cells at 72 h after the start of cell culture in comparison with the intensity at 24 h (Fig. 2B). The fluorescent intensity of ON/GC-5B/KE clone 3 cells was slightly increased at 72 h (approximately four-fold). In contrast to these cell lines, the fluorescent intensity of OGN/GC-5B/KE clone 3 cells did not change during the cell culture. Growth curve analysis of these G418-resistant cell lines revealed that these cell clones had a similar kinetics for cell proliferation, although the growth rate of these cell clones was significantly lower than that of OR6c cells (Fig. 2C). These results suggest that the efficiency of genome-length HCV RNA replication in OGN/C-5B/KE clone 7 cells is higher than that in the other clones. Therefore, we finally selected OGN/C-5B/KE clone 7 (herein designated OGF7) for further characterization.

First, to exclude the possibility that the HCV RNA sequence had become integrated into the genomic DNA, we assayed for the HCV 5′-UTR sequence in the genomic DNA isolated from OGF7 cells by PCR. As a positive control, we used a cloned cell line (Mori et al., 2008) in which the HCV 5′-UTR sequence was integrated into the genomic DNA. The HCV 5′-UTR sequence was not detected in the genomic DNA isolated from OGF7 cells, genome-length HCV RNA-replicating O cells (Ikeda et al., 2005), or OR6c cells (Fig. 3A), although an expected product (266 bp or 205 bp) was detected in the positive control (Fig. 3A, lane PC). These results suggest that the HCV RNA sequence (at least HCV 5′-UTR sequence) is not integrated into the genomic DNA in OGF7 cells. Consistent with these results, an approximately 12 kb RNA of the genome-length HCV RNA encoding EGFP in OGF7 cells was also detected by Northern blot analysis, and its accumulation level was almost the same as that in the O cells (Fig. 3B). In addition, we confirmed by Western blot analysis that OGF7 cells efficiently expressed not only HCV proteins but also the EGFP-Neo^R fused protein, and the expression levels of HCV proteins in the OGF7 cells were also equivalent to those in the O cells (Fig. 3C). In summary, these results indicate that the OGF7 cell line harboring replicative genome-length HCV RNA encoding EGFP as a reporter was stably established.

3.2. OGF7 living cells are useful for direct monitoring of the level of HCV RNA

First, we examined whether or not the expression level of EGFP in OGF7 cells was sufficient to allow direct visualization by confocal laser-scanning microscopy. As a consequence, we could detect the fluorescence in addition to the core protein expressed in OGF7 cells (Fig. 4). Furthermore, we confirmed that the detected fluorescence was derived from the EGFP expressed in OGF7 cells, because both the fluorescence and the core protein disappeared after IFN-α treatment (Fig. 4). These results suggest that the replication of genome-length HCV RNA encoding EGFP-Neo^R fused protein occurs efficiently in OGF7 cells. We next examined whether or not the IFN sensitivity of the EGFP level was associated with that of the HCV RNA level in OGF7 cells. The levels of EGFP and HCV RNA were examined by the fluorometer and real-time LightCycler PCR, respectively. The results revealed that the level of reduction in the fluorescent intensity by IFN-α treatment was equivalent to the level of reduction in the HCV RNA level (Fig. 5A and B). In addition, we confirmed by Western blot analysis that the reduction pattern of the EGFP-Neo^R fusion protein by IFN-α treatment was also similar to those of the core and NS3 proteins (Fig. 5C). These results indicate that the expression level of EGFP is sufficient for monitoring of the level of HCV RNA, and suggest that the direct measurement of the fluorescent intensity of the living OGF7 cells was an effective means of monitoring the level of HCV RNA replication.

3.3. The OGF7 system is useful as a quantitative assay system for various anti-HCV reagents

To clarify whether or not the OGF7 system is useful as a quantitative antiviral assay system, we first compared the IFN-α sensitivity of the OGF7 fluorescent reporter system with that